



Review

Synthesis, Properties, and Biological Applications of Metallic Alloy Nanoparticles

Kim-Hung Huynh ¹, Xuan-Hung Pham ¹ , Jaehi Kim ¹, Sang Hun Lee ², Hyejin Chang ³,
Won-Yeop Rho ⁴ and Bong-Hyun Jun ^{1,*}

¹ Department of Bioscience and Biotechnology, Konkuk University, Seoul 143-701, Korea; huynhkimhung82@gmail.com (K.-H.H.); phamricky@gmail.com (X.-H.P.); susia45@gmail.com (J.K.)

² Department of Bioengineering, University of California, Berkeley, CA 94720-1762, USA; shlee.ucb@gmail.com

³ Division of Science Education, Kangwon National University, Chuncheon 24341, Korea; hjchang@kangwon.ac.kr

⁴ School of International Engineering and Science, Jeonbuk National University, Jeonju 54896, Korea; rho7272@jbnu.ac.kr

* Correspondence: bjun@konkuk.ac.kr; Tel.: +82-2-450-0521

Received: 24 June 2020; Accepted: 18 July 2020; Published: 21 July 2020



Abstract: Metallic alloy nanoparticles are synthesized by combining two or more different metals. Bimetallic or trimetallic nanoparticles are considered more effective than monometallic nanoparticles because of their synergistic characteristics. In this review, we outline the structure, synthesis method, properties, and biological applications of metallic alloy nanoparticles based on their plasmonic, catalytic, and magnetic characteristics.

Keywords: alloy nanoparticles; bimetallic nanoparticles; trimetallic nanoparticles; biological application; synergistic effect; photocatalytic property; super-magnetism

1. Introduction

In principle, nanomaterials indicate materials from subnanometer to several hundred nanometers in size that are applied in material science and nanotechnology due to properties different from those of conventional materials. Metallic nanoparticles are small particles made of metal and can be synthesized by physical, chemical, or biological-based methods. Their properties depend on their composition, size, and shape that determine their plasmonic, catalytic, and magnetic characteristics. Monometallic nanoparticles obtain the property of their constituent metal whereas bimetallic and trimetallic alloy nanoparticles synthesized from two or three metals show more stable structures and enhanced properties. Additionally, alloy nanoparticles demonstrate synergistic effects due to hybrid characteristics such as photocatalytic properties and super-magnetism. Therefore, alloy nanoparticles are being progressively studied for potentially diverse applications. In this article, we summarized and reviewed the results of scientific research over the last 10 years which highlighted the role of alloy nanoparticles in biological applications such as bio-imaging, sensors, catalyst, drug delivery, and therapies as well as their types, synthesis, and properties.

2. Classification of Alloy Nanoparticles

According to atomic ordering, bimetallic nanoparticles can be classified into four types [1,2]:

2.1. Mixed Alloyed Nanoparticles

They may have a random or ordered arrangement (Figure 1a). Randomly mixed nanoalloys are often termed alloyed nanoparticles, whereas ordered mixed nanoalloys are termed intermixed or intermetallic nanoparticles [3].

2.2. Sub-Cluster Segregated Alloyed Nanoparticles

These nanoparticles comprise two small clusters (sub-clusters) in their structure (Figure 1b). There are two kinds of sub-clusters. One shares the middle interface whereas the other only shares a bone or short interface between two small clusters [4].

2.3. Core-Shell Alloyed Nanoparticles

These nanoparticles typically consist of one metal that forms a shell surrounding a core made of another metal or the recent core–shell type which is composed of an intermixed core surrounded by a pure shell [5]. This type is created more commonly and has diverse applications [6] (Figure 1c).

2.4. Multiple Core-Shell Alloyed Nanoparticles

These have two further kinds of multiple arrangements, multiple shell–core nanoparticles created with two or more shells covering a single core, and multiple core–shell nanoparticles with one simple shell surrounding several cores; the shell and core are always composed of two different metals [7–12] (Figure 1d).

The degree of mixing and atomic ordering in bimetallic nanoparticles can be controlled by the relative strength of the bond between two chemicals, the surface energy, atomic size, electric or magnetic effects, etc. [1].

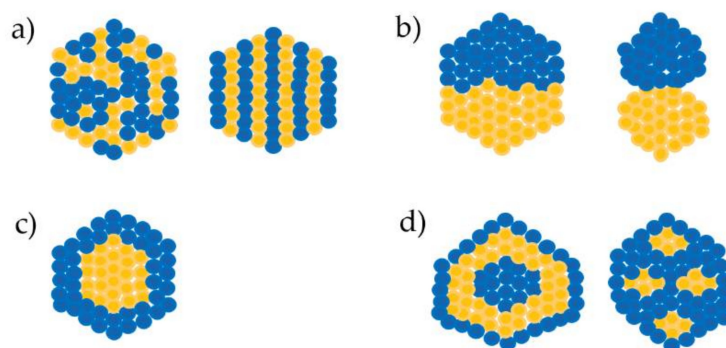


Figure 1. Types of bimetallic alloyed nanoparticles. (a) Mixed alloyed nanoparticles; (b) Sub-cluster segregated alloyed nanoparticles; (c) core-shell alloyed nanoparticles; (d) multiple core-shell alloyed nanoparticles [1,2].

Trimetallic nanoparticle types are similar to those of bimetallic nanoparticles. These are mixed alloyed nanoparticles with a mixture of three metals and core–shell alloyed nanoparticles with a mixture of two kinds of chemicals in the core with a single chemical in the shell or simply one chemical in the core with a mixture of two chemicals in the shell. Another type of trimetallic nanoparticles is the separate core–shell type in which each of the three chemicals sequentially form the core–shell–shell [13–20].

3. Methods of Synthesizing Alloy Nanoparticles

There are two basic ways to synthesize nanoparticles: the top-down approach and bottom-up approach. The top-down approach involves the production of nanoparticles from macro-sized materials, whereas the bottom-up approach involves the creation of nanoparticles from atoms. Between both methods, the bottom-up method is more popular and developed, and generally relies on synthesis

pathways of two main categories: simultaneous method and successive method. The simultaneous method demands precursor materials of the metals of interest (which can be bimetallic or trimetallic alloy clusters) in the same reaction. The successive method involves the growth of particles by reducing metal ions over the surface of another metal core [2,21].

3.1. Physical Methods-Based Nanoparticle Synthesis

3.1.1. Sputtering

Sputtering is a procedure in which nanoparticles are created by bombarding the target metal with high energy [1]. Atom beam sputtering involves three basic steps: migration of atoms from the surface of materials, nucleation and growth of nanoparticles, and absorption onto another material in an electric field [22–24]. Magnetron sputtering involves sputtering in a magnetic field, in which one or more materials are deposited on the surface of another material such as metal or ceramics through a high-rate vacuum coating technique [25–29]. This method can provide high purity but it is difficult to control the morphology of the nanoparticles formed; moreover, its energy requirement is too high, which can pose a danger [30]. There are many studies on making thin films with alloy nanoparticles on the surface using the sputtering method, such as Au–Ag alloy nanoparticles in SiO₂ or TiO₂ thin films [25,27,28].

3.1.2. Thermal Decomposition

Thermal decomposition-based methods synthesize nanoparticles based on temperature. Synthesis of transition metal nanoparticles such as Fe, Ni, and Co requires high temperatures because these metal nanoparticles are not stable at room temperature. This method is also applied for metals that have low reduction potential or difficult reduction characteristics. The process starts with forming particles of the metal precursor having lower decomposition temperature, followed by the next metal precursor that decomposes when the temperature is increased [2,31,32]. This method is used for fabricating good quality crystals or commercial value crystals. The main disadvantage of this technique is the need for high temperatures, which can be dangerous, and difficulty in isolating unstable nanoparticles from the reaction at high temperature [30,33]. Fe-, Ni-, and Co-based alloy nanoparticles such as Pt–Co, Au–Fe, Au–Ni, Au–Co, Fe–Co, Fe–Ni, Co–Pt, Ni–Mo, Pt–Ni–Fe, Sn–Zn–Cu, and Au–Cu–Pt are produced by thermal decomposition [14,20,34–44].

3.1.3. Radiolytic Method

Fabrication of metal nanoparticles by irradiation is called radiolytic synthesis. In this case, the gamma (γ) ray or electron beam is used to reduce metal ions in soluble precursors thus forming metal nanoparticles. This method can produce alloy nanoparticles that are not stable when created by thermal decomposition. The type of alloy nanoparticle created depends on the dose of irradiation. A low dose can lead to the creation of core–shell alloy nanoparticles whereas a higher dose controls the making of mixed alloy nanoparticles [45–48]. The difficulty of the radiolytic method is in directing the nanoparticles' shape. However, irradiation-based techniques are low-cost, environment-friendly, and show promise for large applications [2,49–51]. There are many examples of the alloy nanoparticles fabricated based on radiolytic synthesis, such as Rh–Pd, Rh–Pt, Au–Ag, Au–Pt, Au–Pt–Ag, Pt–Ru–Sn, Pd–Ru–Ni, and Zr–Ni–Cu alloy nanoparticles [46,52–61].

3.1.4. Sonochemical Synthesis

The sonochemical synthesis method is based on ultrasound. In solution, ultrasound can cause high temperature or high pressure. Due to the increased temperature, small metal nanoparticles are created at a rapid reaction rate. Ultrasound induces the collapse or formation of tiny bubbles in a solution that allows the creation of hollow nanoparticles. Further, the production of oxidizing and reducing radicals is crucial for the synthesis of metal nanoparticles [62–65]. Figure 2 showed brief schematics of the

sonication reactor. Sonochemical synthesis has been in use for more than twenty years to synthesize bimetallic alloy nanoparticles such as Au–Pd nanoparticles [66] and has been recently combined with other techniques for the creation of alloy nanoparticles [67,68]. Various alloy nanoparticles such as Au–Pd, Co–Cu, Fe–Pt, Hg–Pd, Au–Ru, Pt–Cu, Fe–Ag–Pt, Pd–Co–Pt have been manufactured by using sonochemical synthesis method [13,66,67,69–75].

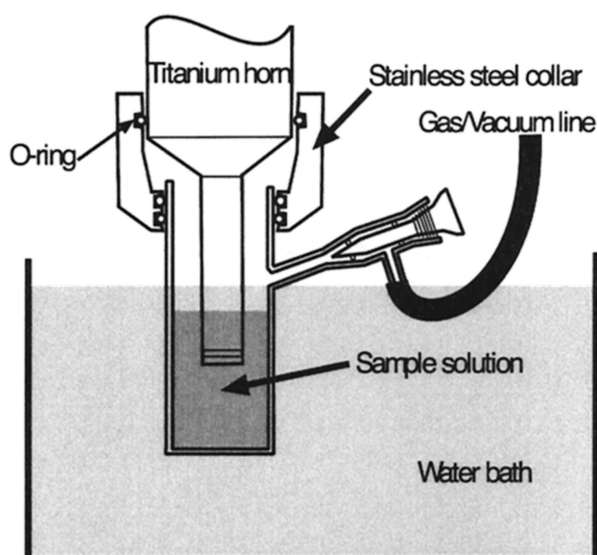


Figure 2. Schematics of the sonication reactor [62].

3.2. Chemical-Method Based Nanoparticle Synthesis

3.2.1. Chemical Reduction

The chemical reduction method is used for producing bi-/tri-metallic alloy nanoparticles through the reduction of appropriate precursors to the zero-valent state. This method involves two phases, reduction and growth. The reduction process occurs sequentially: at first, the metal precursors owning to the highest redox potential precipitate to form the core, followed by the second and possibly third precursor being deposited as a shell [1,31,33,76,77]. Organic solvents are used to prevent agglomeration and maintain the stability of nanoparticles in the solution phase [78–81]. The advantages of the co-reduction technique include simplicity of steps and versatile application but still has the disadvantage of presence of impurities; for instance, the Au–Pd–Pt trimetallic alloy nanoparticle created by simultaneous reduction of multiple metal precursors had an Au core with a mixed Pd and Pt shell that was not separated into two separate layers as the Pd shell and Pt shell [17]. Due to its simplicity, bimetallic (Pt–Ag, Pt–Co, Pt–Au, Pd–Ag, Pd–Pt, Au–Ag, Au–Pt, Ag–Au, Ag–Co) and trimetallic (Pt–Pd–Co, Co–Ni–Cu, Ni–Au–Pd, Pd–Pt–Ni, Au–Pd–Pt) alloy nanoparticles have been produced by this method and will be further improved in future [78,81–92].

Galvanic displacement reactions are possibly considered as a chemical reduction subsection that is used to produce bimetallic hollow and porous nanoparticles [93]. This method is the replacement reaction which is based on electrical potential difference between two metals that are templates and a salt precursor in a suspension [94]. This is common in creating a metallic shell coating the metallic excited core of nanostructures with a large range of various morphologies such as nanospheres, nanoboxes, nanorings, nanotubes and nanocages [94,95]. Ni–Pt, Au–Ag and Cu–Ag nanoparticles are examples that are produced by galvanic displacement method [96–98].

3.2.2. Electrochemical Synthesis'

Electrochemical synthesis uses electricity as the main source of composite reactions. This method is mostly used in industrial applications. An electrical field is created by two electrodes. Reduction occurs at the metallic anode or with the anode itself dissolved in solution along with the metal precursor, and new metallic nanoparticles are formed at the cathode. A stabilized chemical for stabilization of fresh metal particles has to be included there. This method has advantages of controlling the nanoparticle size, imparting high purity, and being environmentally-friendly and cost-effective [1,16,30,99]. Therefore, this technique is applied in the large scale manufacture of many bimetallic (Rh–Pd, Au–Pt, Pt–Au, Ag–Au, Cu–Ag, At–Ni) and trimetallic (Pd–Fe–Ni, Pd–Ag–Cd) alloy particles [16,19,100–111].

3.2.3. Hydrothermal Methods-Based Nanoparticle Synthesis

In this method, nanoparticles are synthesized in high-temperature aqueous solutions at a high vapor pressure. Although this method allows monitoring of the nanoparticle growth, and their physical and chemical properties, its disadvantages include high-temperature conditions and high-cost equipment [30,112,113]. Many bimetallic nanoparticles such as NiFe_2O_4 (nickel ferrite), co-doped $\text{Zn}_{1-x}\text{Co}_x\text{Mn}_2\text{O}$, Ni–Cu, Au–Cu, Ag–Co, Ni–Fe, and Co–Ni nanoparticles are created using the hydrothermal method [114–119].

3.2.4. Chemical Precipitation-Based Nanoparticle Synthesis

Chemical precipitation involves the formation of solids from a solution by creating a supersaturated condition or by converting the soluble material into an insoluble form via pH change, electrooxidising potential, or adding of a precipitation reagent [30,120,121]. A typical chemical precipitation method contains four stages: precipitation, flocculation, sedimentation, and solid-liquid separation [121]. This method is a single-step process that is useful in large-scale production of nanoparticles. Chemical precipitation is popularly utilized in water purification [30,120,121]. Some studies have reported the fabrication of Mg–Zn, Pd–Fe, and Fe–Ni–Ce alloy nanoparticles by the chemical precipitation method [122–124].

3.2.5. Other Chemical Methods of Nanoparticle Synthesis

The above-mentioned methods involve synthesis in homogeneous liquids such as water or organic solvents; however, there are other synthesis methods that use the gas phase or heterogeneous phases such as sol-gel and micro-emulsion.

There are some methods by which metal nanoparticles are synthesized in a gaseous environment such as the selective catalytic reduction method and flame spray pyrolysis. In the flame spray pyrolysis method, a metal precursor solution that is sprayed is reduced by temperature, turning into a metal particle [125,126]. In the selective catalytic reduction technique, the reaction changes nitrogen oxides using a gaseous catalyst such as urea and ammonia [33,127].

The sol-gel approach involves the basic steps of hydrolysis, condensation, and drying. There are two types, aqueous sol-gel in which the solvent is water, and nonaqueous sol-gel in which the solvent is an organic solvent. This method is simple, economical, and can be processed at low temperature [67,127–134].

The micro-emulsion method, in its simple definition, is a system comprising three components: a minor droplet (dispersed phase), an immiscible solvent (continuous phase), and a surfactant that covers the droplet. Depending on the properties of the dispersed phase, continuous phase, and the hydrophilic-lipophilic balance value of the surfactant, there are many types of micro-emulsions, such as water-oil, oil-water, and water-Triton X-100 among others. The metal nanoparticles are synthesized inside droplets that can be designed to the desired size and composition. This method has been applied broadly in the synthesis of bimetallic and trimetallic alloy nanoparticles [135–143].

3.3. Biological Methods of Nanoparticle Synthesis

Since the development of nanotechnology, many approaches for nanoparticle synthesis have been discovered and improved. Most of these are chemical methods based on hazardous chemicals, enormous energy, and high temperature and form nanoparticles with limited properties. To overcome these disadvantages, green synthesis approaches, such as those based on microwave, electrochemical, hydrothermal, and sonochemical methods have been developed. Another green synthesis method that has progressed recently is based on biological sources such as plants, microorganisms, and industrial and agricultural wastes [144–148]. Biological synthesis has been applied to a large extent in nanoparticle production and has also been used for fabricating bimetallic or trimetallic alloy nanoparticles.

3.3.1. Microorganisms to Produce Nanoparticles

Micro-sized organisms, including bacteria, fungi, yeasts, and even viruses have been considered as nano-factories to produce nanoparticles (Figure 3) because of their ability to accumulate and detoxify heavy metals via various reductase enzymes [149]. The metal reduction can be carried out in the extracellular or intracellular environment. The genes, proteins, enzymes, and biomolecules of the microorganisms play roles as reducing factors. Bacteria such as *Escherichia coli*, *Salmonella typhimurium*, *Listeria monocytogenes*, *Bacillus subtilis*, and *Rhodospseudomonas capsulata* [150–157] have been used to create Au–Pd, Pd–Pt, Pd–Ag, Au–Ag, Pd–Fe, Au–Fe, Pd–Au–Fe, and Cu–Ag alloy nanoparticles.

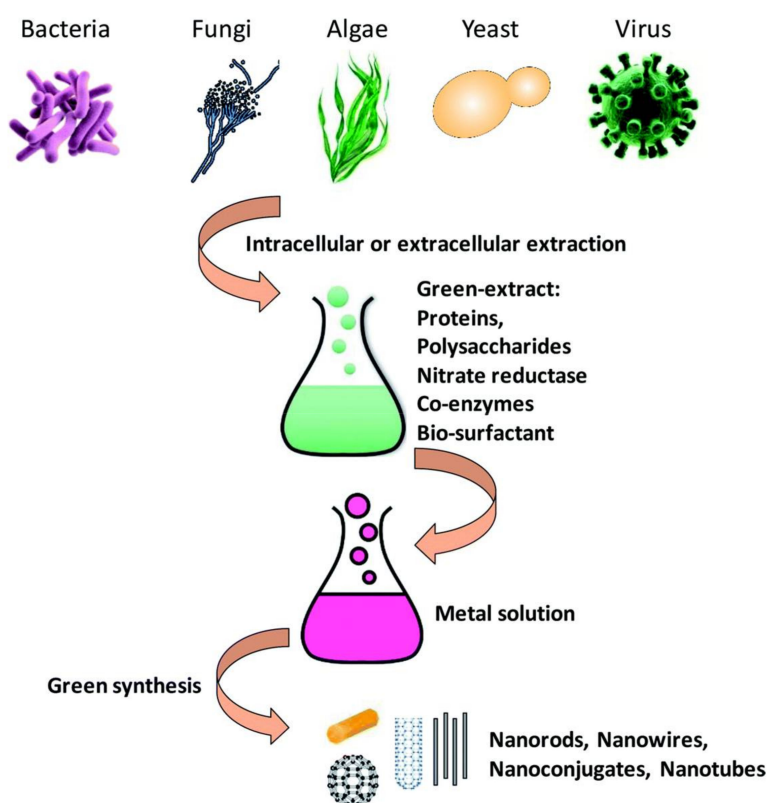


Figure 3. Schematic of metal nanoparticle synthesis by microorganisms [149].

Fungi and yeasts have been used for nanoparticle synthesis. Compared to bacteria, they have some advantages such as high accumulation, high yield, easy to culture, and presence of complex proteins that help in nanoparticle synthesis. When fungi are exposed to a metal ion environment, they produce compounds or biomolecules such as naphthoquinones, anthraquinones, or nitrate reductase as reducing factors to create metal particles [144,145,158,159]. Fungi such as *Fusarium semitectum*, *Neurospora crassa*, *Fusarium oxysporum*, *Pleurotus ostreatus*, *Coriolus versicolor* and yeasts such as *Saccharomyces cerevisiae*,

Schizosaccharomyces, *Schizosaccharomyces pombe*, and *Candida glabrata* have been used to manufacture Au-Ag and Cd-S alloy nanoparticles [160–170].

Viruses, which are not considered as a complete living organism, are also utilized in nanomaterial synthesis. Particularly, plant virus capsids work as a useful bio-template in nanoparticle production [171–173]. Some plant viruses (Cowpea mosaic virus, tobacco mosaic virus, Red clover necrotic mosaic virus) have been used in producing Fe–Pt, Co–Pt, Co–Fe, Cd–Se alloy nanoparticles [174–176].

3.3.2. Plants as Source of Nanoparticles

Recently, plants have been explored as an option for the green synthesis of nanomaterials. It involves the application of various plant organs such as the root, stem, leaf, seed, fruit peel, and flowers and their extracts to manufacture nanoparticles. This method is eco-friendly and stable, and the created nanoparticles have potential use in biomedical and environmental applications. It is proposed that plant constituents, including protein, amino acids, organic acid, and polysaccharides, and secondary metabolites such as polyphenols, flavonoids, alkaloids, heterocyclic, and terpenoid compounds play roles as reducing agents and stabilizing factors [144,145,177,178]. Monometallic nanoparticles as well as metallic alloy nanoparticles have been manufactured using plant-based approaches. For instance, Ag–Ni, Ag–Co, Pt–Cu, Au–Ag, Ag–Cu, and Zn–Ag nanoparticles have been produced using the leaf extracts of *Canna indica*, *Alchornealaxiflora*, *Azadirachta indica*, *Cacumen Platycladi*, palm, *Mirabilis jalapa*, and *Moringa oleifera* [179–185], Au–Ag–Sr, and Fe–Ag–Pt nanoparticles were produced from the roots of coriander, *Platycodon grandiflorum* [13,186], and Au–Ag nanoparticles have been produced from the Chinese wolfberry fruit extracts [187].

Algae are small eukaryotic organisms also used for the synthesis of alloy nanoparticles; for instance, *Phaeodactylum tricornutum*, *Chlamydomonas reinhardtii*, and *Spirulina platensis* were utilized to prepare CdS and Au–Ag nanoparticles [188–190].

3.3.3. Agricultural and Industrial Waste as Source of Nanoparticles

In recent years, nanoparticles have been synthesized largely from agricultural and industrial wastes (Figure 4). Post-harvest wastes such as fruit peels, rice husk, and egg shells form approximately 80% of the biomass on the field, and industrial waste such as timber dust, sugar cane bagasse, and wild weeds including unwanted plants, herbs, or shrubs that are usually burned, can be used as biological sources for the green synthesis of nanoparticles. The use of these waste materials compared with the physical and chemical methods has benefits including reduction of using harmful chemicals, low-cost, low energy, and renewing waste material [191–195]. Many monometallic nanoparticles were manufactured using citrus fruit peel extract, grape waste, mango peel, rice husk, sugar cane bagasse and leaves, bamboo leaves, egg shell, and coconut shells. Moreover, Au–Ag and CdS alloy nanoparticles were also manufactured using banana peels and the otherwise useless weed *Antigonon leptopus* [196–198].

Typically, biological synthesis depends on pH, temperature, pressure, time, and protocol. It has plenty of advantages such as being an ecofriendly, low-cost, safe, and simple method that requires a short time. The biosynthesized nanoparticles have biocompatible characteristics and can be introduced into biological and pharmacological applications without an additional step of attaching to bioactive compounds. However, these synthesis methods also have some disadvantages due to the complicated parameters or complex constituents in plant organs; the size and shape of nanoparticles can be seldom controlled well. In some cases, the generated nanoparticles cause toxicity to the plant, and bacteria [149,199].

Nowadays, alloy nanoparticles with supports like carbon, silica substrates, and graphene sheets among others are being increasingly manufactured, thereby generating a variety of useful of nanoparticles.

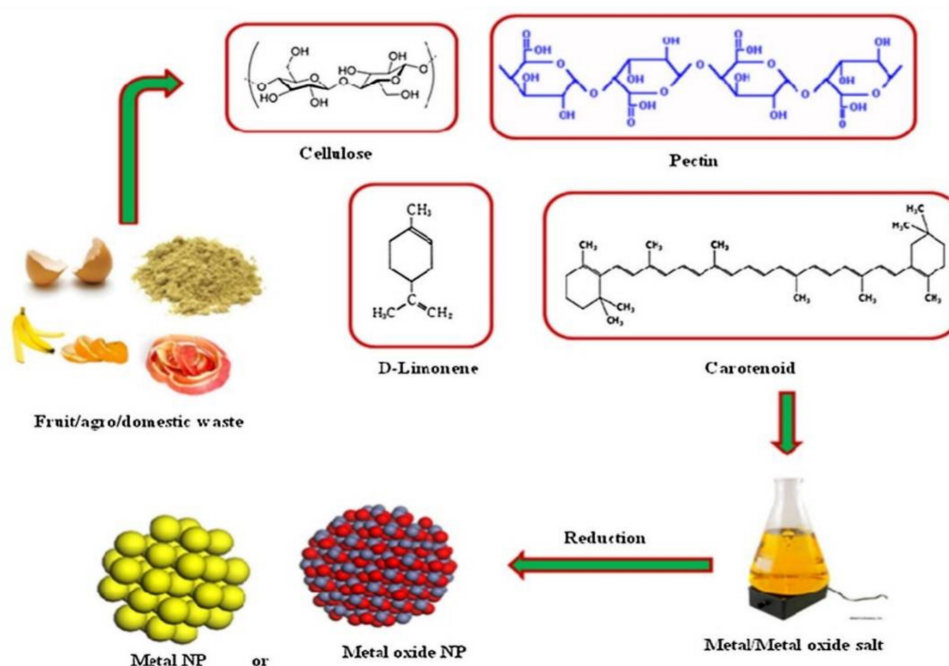


Figure 4. Synthesis of nanoparticles using waste materials [195].

4. Properties of Alloy Nanoparticles

The most distinctive feature of bimetallic or trimetallic alloy nanoparticles is the combination of physicochemical properties of the chemicals from which they are created. Typically, there are three main metal groups based on their characteristics: Cu, Ag, Au for plasmonic; Pd, Pt, Ru, and Rh for catalysis; and Fe, Ni, Co for magnetism. Combining two or more metals almost always increases the inherent characteristics. For example, the Au–Pt bimetallic nanoparticles composed of plasmonic Au and catalytic Pt have a hybrid property of catalytic ability that can be boosted by light [31].

4.1. Catalytic Properties

Many studies have shown that alloy nanoparticles are more active than monometallic nanoparticles made with the same metal. The catalytic properties of bimetallic nanoparticles depend on the structures that are different between the core–shell structure and the disordered structure and composition of alloy nanoparticles. Pt–Ni alloy nanoparticles catalyze the oxygen reduction reaction ten times faster than Pt nanoparticle [200]. Another report showed that Pt–Ru alloy and Pt–Ru core–shell nanoparticles show differences in catalytic reactions [201]. Further, among core–shell bimetallic nanoparticles, the catalytic activities are different as indicated in the study by Tsang’s group; they showed that the catalytic action of M–Pd core–shell nanoparticles (M = Rh, Pt, Ru, Au, Ag) in formic acid decomposition increased linearly with the increasing of difference in charge density between the core metal and the shell [202]. The thickness of the shell also affects the catalytic activity [203].

4.2. Photocatalytic Properties

Photocatalytic characteristics are a great advantage of alloy nanomaterials composed of a plasmonic metal and catalytic metal, such as Au–Pd, Ag–Pt, and Cu–Pd nanoparticles. Photocatalysis occurs with visible or ultraviolet light, which is absorbed and subsequently released as energy that facilitates catalysis. Some reports indicate that plasmons support chemical transformation. Further, thermal assistance is more effective for photocatalysis [31,204–206].

4.3. Optical Properties

Localized surface plasmon resonance (LSPR) is an optical property of nanoparticles. Among metals, Au, Ag, Cu, Pd, and Pt have attracted much attention due to their optical properties that are largely applicable in photocatalysis, biomedicine, Surface-enhanced Raman spectroscopy (SERS), and photothermal therapy. Optical properties depend on the size, shape, and composition of nanoparticles [207]. Some studies have shown that LSPR peak position, intensity, and line width is influenced by the size of nanoparticles. For example, by decreasing the size of Au nanoparticles, the emission light position changes from the NIR region to the UV region. Due to a very small size, nanoparticles can lose their LSPR and become photoluminescent [208–212]. In addition, LSPR sensitivity is highly dependent on the shape of nanoparticles. One study reported that the sensitivity of Au nanoparticle increased in the order of spheres, cubes, shells, rods, rattles, stars, branches and rings [31].

The optical property of bimetallic nanoparticles is strongly affected by their component metals. LSPR increases in the case of combining two plasmonic metals being resonant in the visible region (Au–Ag, Au–Cu nanoparticles), whereas it decreases or quenches if one metal in the combination is resonant in the UV region (Pd, Pt) like Ag–Pd nanoparticles. In core–shell alloy nanoparticles, LSPR is also affected by the shell metal. With increasing thickness of the shell, the LSPR peak position moves directly from the peak position of the metal forming the core to the peak position of the shell metal [31,213].

4.4. Magnetic Properties

Compared to monometallic nanoparticles, bimetallic nanoparticles have an extra useful feature of the magnetic property. According to Bansmann's group, a mixture of 3d metals (Fe, Ni, etc.) with big local magnetic moments and 4d or 5d metals (Pd, Pt, etc.) with strong spin-orbit coupling creates bimetallic nanoparticles with high magnetic moments and large anisotropy [214]. Further, Pt-based nanoparticles have additional properties such as oxidation resistance and catalysis. In summary, combination of these metals to produce alloy nanoparticles results in more effective magnetism, better stability, and additional catalytic characteristics [31,214].

5. Application of Alloy Nanoparticles in the Biological Field

Similar to monometallic nanomaterials, bi and trimetallic alloy nanomaterials are used in a large range of biological applications. Moreover, alloy nanomaterials show interesting synergism in the properties of the metals from which they are created. This allows alloy materials to be used more effectively. Here, we discuss the bio-application of alloy nanoparticles in imaging, diagnosis, and therapies.

5.1. Imaging

Researchers always aim towards a better understanding of the structure as well as the function of living organisms. This requires high-quality bioimaging at various levels ranging from molecules, cell, organs, to the whole body. Microscopy and many different methods have long been used to capture the images of the cells or whole body of organisms. Nanomaterials that have optical properties are widely applied in bioimaging. Until now, there have been many studies about using plasmonic nanoparticles like Au nanoparticles and quantum dots in imaging cell components, surface species, endocytic pathways, cell cycle and apoptosis processes, cell secretion, animal organs, and microorganisms [215–217]. Nanoparticles acting as bioimaging probes possess characteristics such as the ability to penetrate into cells, good analytical signals, solubility and stability in relevant solvents or intracellular environments, ability to attach with functional groups for site-specific labeling, and low cytotoxicity [218]. Au and Ag-based bimetallic nanoparticles have been developed for cell imaging. For instance, Ag–Au nanoparticles or porous nanospheres combined with biomolecules exhibit enhanced optical properties, good dispersion in aqueous solution, high physiological stability,

and favorable biocompatibility and were used as a label probe [219,220]; Zn doped Ag nanoclusters with L- cysteine and chicken egg white showed an increased quantum yield compared with pure Ag nanoclusters; moreover, they showed excellent stability in their role as a probe in the imaging of fungal cells (*Alternaria* sp.) [221] (Figure 5). Cu-doped Au nanoclusters exhibited fluorescence intensity that decreased linearly with increasing Cu concentration but exhibited higher photostability than Rhodamine 6G (conventional fluorescent dyes) at 24 h in ex vivo as observed in self-illuminating NIR images of major organs (tumor, heart, liver, spleen, lungs, and kidneys) from U87MG tumor-bearing mice [222].

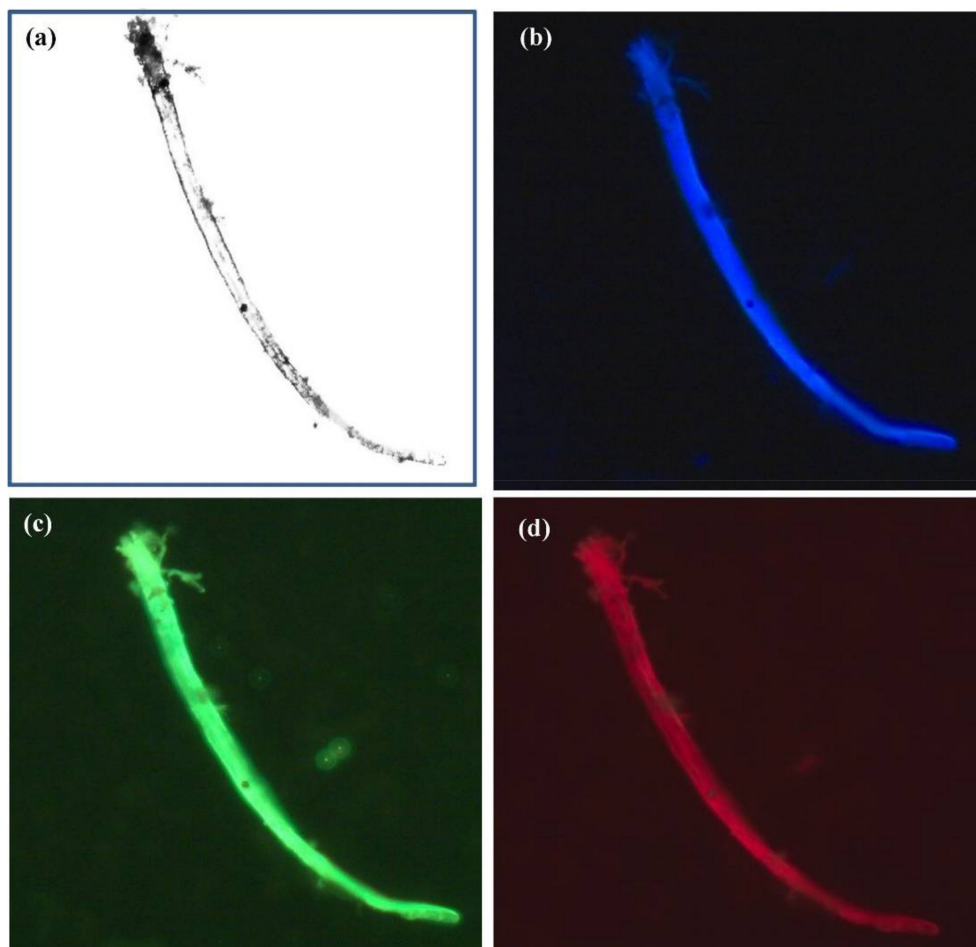


Figure 5. Fluorescence microscopic images of fungal cells (*Alternaria* sp.) treated with chicken egg white-L-Cysteine-encapsulated Zn-undoped Ag nanoclusters. Image (a) without chicken egg white-L-Cysteine-encapsulated Zn-doped Ag nanoclusters and images with chicken egg white-L-Cysteine-encapsulated Zn-undoped Ag nanoclusters upon the laser excitation at (b) 405 nm (blue), (c) 488 nm (green), and (d) 561 nm (red), respectively. The concentration of chicken egg white-L-Cys-encapsulated Zn-undoped Ag nanoclusters was 0.5 $\mu\text{g/mL}$ [221].

5.2. Diagnosis

5.2.1. Biomedical Imaging

Bioimaging is used for the recognition of shapes, structures, and pathways in organisms as well as in disease diagnosis, especially in cancer and tumor detection. Gold and iron-based nanoparticles and quantum dots are used in many biomedical imaging techniques such as magnetic resonance imaging (MRI), computed tomography (CT), photoacoustic (PA) imaging, high-order multiphoton

luminescence (HOMPL) microscopy, contrast-enhanced dual-energy mammography (DEM), and so on for cancer and tumor detection [223,224].

To overcome the disadvantages of nanoparticles like brightness, alloy nanoparticles have been demonstrated to possess superior qualities in biomedical imaging. Iron-based alloy nanoparticles such as Fe–Ni, Fe–Pt are utilized in magnetic resonance imaging as potential contrast agents that show a high magnetic or superparamagnetic property, along with low toxicity in living cells [224–227].

According to the study by Cormode and group, Au–Ag alloy nanoparticles are applied in dual-energy mammography (DEM) or computed tomography (CT) as imaging probes for breast cancer screening [228]. The gold in the alloy nanoparticle reduces the leaching of silver from the particle and increases biocompatibility. In an in vivo experiment, the Au–Ag nanoparticle showed a clear contrast in the tumor when analyzed by the DEM and CT techniques. Therefore, Au–Ag nanoparticles are a prospective contrast agent for breast cancer detection by DEM and CT [228].

5.2.2. Sensors

The superb plasmonic property of Ag- or Au-based alloy nanoparticles allows their applications as sensors using the SERS technique or fluorescence with a variety of detected targets like metal ions, chemicals, and biomolecular targets [229]. For example, using a keratin template, Ag–Au nanoclusters have been fabricated for mercury ion detection. The alloy material shows approximately five-fold higher fluorescence than that with Au nanoclusters with keratin. This proved that Ag addition supports the fluorescence intensity and makes the alloy cluster more stable. Thereby, mercury ions were detected in a wide range with low detection limits [230]; AuM (M can be Pd, Pt, Rh) nanoparticles show remarkably enhanced hydrogen peroxide (H₂O₂) detection when compared with Au, Pt, Rh, Pd monometallic nanoparticles [231], and Au–Ag, Ag–Pd, Ag–Pt bimetallic nanoparticles are utilized in detection of biomolecules such as glutathione, cysteine, endonuclease, L-cysteine, and adenine with ultra-bright fluorescence or SERS intensity [232–236].

Immunofluorescence technology using quantum dots as beneficial reporters exhibit properties such as sensitivity, high specificity, and fast results due to the characteristics of quantum dots including higher photoluminescence and quantum yields, higher optical and chemical stability, and broader emitting range. Especially, alloy quantum dots have improved photoluminescence intensity and stability compared to standard quantum dots. Therefore, they have been widely used in clinical diagnosis, clinical analysis, and cancer detection [237–239]. For instance, ZnSe/CdS/ZnS core–shell quantum dots have been used in the detection of C-reactive protein, an early indicator of infection and autoimmune disorders [237]; bovine serum albumin-doped CdS quantum dots have been used in detecting human IgG1, a low-abundance protein [240]; Cu:ZnInS/ZnS quantum dots have been used in tetanus antibody detection [241]; CdTe quantum dots are used for detecting α -fetoprotein, a tumor marker [242]; and S- and N-Co-doped carbon quantum dots have been used in detecting clenbuterol, a feed additive for livestock and poultry [239].

5.2.3. Catalyst

Nanoparticle-based catalysts are structured with catalytically efficient metals such as Pd, Ni, and Pt. Similar to other alloy nanomaterials, catalysts like Pd–Ru and Pd–Co, made of bimetallic nanomaterials have excellent hybrid catalytic characteristics and exhibit photocatalysis when combined with metals with optical properties like Pt–Au [243,244]. Bimetallic catalysts thus show higher catalytic activity and longer stability than monometallic catalysts.

For example, between Pd–Ru nanoparticles and Ru nanoparticles produced by *Bacillus benzeovorans*, Pd–Ru nanoparticles show better catalytic activity than Ru nanoparticles in converting 5-hydroxymethyl furfural (5-HMF) to the fuel precursor 2,5-dimethyl furan (2,5-DMF) [243]. In methanol and ethanol electrooxidation, Pd–Co nanoparticles supported on graphene show a slight decrease in catalysis but show strong stability, long term use, and magnetic property that allows easy separation from a mixture compared with Pd nanoparticles supported on graphene. Further, Pd–Fe, Pd–Zn, Ni–Fe,

Pt–Fe, and Ag–Pd nanoparticles exhibited more effective catalysis of chlorinated organic solvents and chlorinated aromatic compounds [245,246]. The photocatalytic activity of CuAu–ZnO–Graphene nanocomposite and Au–Pt–TPAD (triphenylamine derivative, 2,2'-(4-(4-(diphenylamino) styryl) benzylazanediy) diacetic acid (TPAD)) (Figure 6) was higher than the catalytic activity of the respective monometallic nanomaterial [247,248].

Trimetallic nanomaterials show superior catalytic activity compared to bimetallic or monometallic nanoparticles. Various studies have reported that Ag–Au–Pt and Au–Pd–Pt trimetallic nanoparticles possessed superb catalytic activity in methanol oxidation that are not seen with Pd–Pt, Au–Pt, and Pt–C bimetallic nanoparticles or with Pt and Au monometallic nanoparticles [17,249,250].

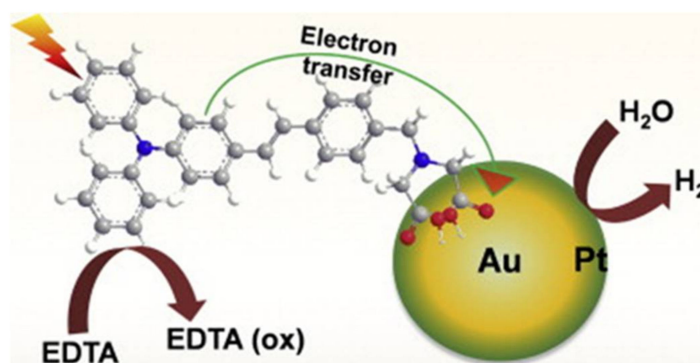


Figure 6. Schematic representation of electron transfer from a triphenylamine derivative, 2,2'-(4-(4-(diphenylamino) styryl) benzylazanediy) diacetic acid (TPAD) sensitizer into an Au core–Pt shell nanoparticle and photoinduced hydrogen evolution under light irradiation [248].

5.3. Therapy

5.3.1. Drug Delivery and Cancer Therapy

In therapy, the aims of drug delivery include precise targeting (target infected cells but not healthy cells), therapeutic efficacy, and low cytotoxicity, whereas conventional drug delivery systems pose challenges such as poor specificity, low therapeutic activity, and toxicity. Modern drug carriers exhibit satisfactory characteristics of specific targeting, controlled drug release, and less toxicity, and are called smart carriers [251–253]. Drug carriers are fabricated using organic materials (polymeric micelles, solid lipid, liposome, and dendrimer) or inorganic materials (silica nanoparticles, Au nanoparticles, magnetic nanoparticles, quantum dots, carbon nanotubes, and nanographene) [253,254] and are discussed in detail in this review.

Inorganic carriers are typical core–shell structures (Figure 7). Their core part can be made of gold, quantum dots, or silica, whereas the shell part contains organic polymers, ligands that provide biocompatibility, and protection that help carriers to easily infiltrate the biological environment of the human body. The properties of carriers are tuned by composition, shape, size, and surface modifications. In addition, they have the novel property of controllable delivery and release in response to a variety of stimuli such as light, pH, temperature, magnetic force, enzyme reaction, among others. They can carry many kinds of therapeutic molecules including anticancer drugs (doxorubicin, paclitaxel) RNA, DNA, proteins, and antibodies [253,255].

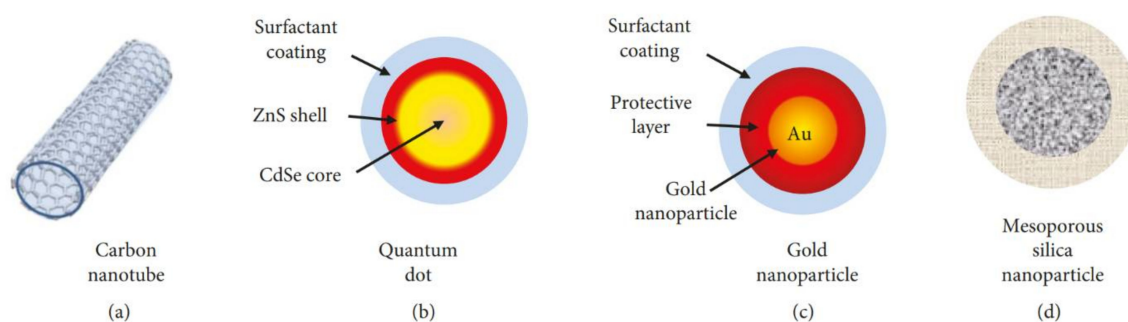


Figure 7. Example of the most employed inorganic nanocarriers: (a) carbon nanotubes, (b) quantum dots, (c) gold nanoparticles, and (d) mesoporous silica nanoparticles [253].

Besides being a drug carrier, these inorganic carriers can also act as therapeutic agents, especially in cancer therapies such as radiotherapy, magnetic hyperthermia therapy, photodynamic therapy, and photothermal therapy [254].

Gold-based nanoparticles are a good candidate for cancer therapy due to their brilliant properties. Gold nanoparticles are nontoxic for some human cells, which is beneficial for intracellular treatment. The negative charge helps gold nanoparticles acquire bio-functionality in conjugation with various functional molecules such as DNA, protein, and antibodies. Further, gold is a radiosensitizer that can convert light to heat that can be used in cancer treatment [253,254]. One report said that the irradiation of gold nanoparticles induces transient changes locally of cell membrane permeability in biological environment that can support the design of new drug delivery systems [256]. Another report also showed that Ag–Au alloy nanoparticles exhibited hepatoprotective activity against diethylnitrosamine (DEN)-induced liver cancer in a Sprague Dawley rat model [257]. Gazouli et al. demonstrated that Ag–Au (ratio 3:1) alloy nanoparticles synthesized by a chemical reduction method could prevent excessive tryptophan-induced apoptosis in cancer cell lines, HCT116 (colon cancer cells), 4T1 (highly metastatic breast cancer cells), and HUH7 (hepatocyte-derived carcinoma cell line) via p53, CASPASE-3, and BAX/BCL-2 pathways [258]. Another study about the inhibitory effect of the ordered topology of Ag–Au alloy nanoparticles on mouse Lewis lung carcinoma indicated that Ag core–Au shell type particles with a 1:1 ratio possessed the best antitumor activity and lowest toxicity among other types of alloy nanoparticles including, Ag core–Au shell and Au core–Ag shell particles with different ratios [259].

Quantum dots are semiconductors with fluorescence properties that allow them to be used for real time drug delivery and as photosensitizers. With surface modification using tumor recognized molecules and drugs, quantum dots can move to target tumors and act as a supporting energetic agent in photodynamic therapy, a method that combines light and photosensitizers to generate oxygen species and promote tumor suppression [254,260–262]. Quantum dots are frequently used in a complex like with graphene and photosensitizer such as chlorin e6 [261,263]. Martinenko et al. reported that the complex ZnSe/ZnS quantum dots with chlorin e6 showed two-fold enhancement of photodynamic destruction in Ehrlich ascites carcinoma cells compared to that with free chlorin e6 molecules, and approximately 50% fluorescence resonance energy transfer from QDs to the chlorin e6 molecules [264].

Hyperthermia therapy is based on heat. The temperature in tumor cells is increased to 40–45 °C for inducing certain pathways including apoptosis. Magnetic nanoparticles can be heated under the magnetic field leading to direct killing of cancer cells, or by releasing the carried drug to kill the cancer cells [265,266]. Many kinds of magnetic nanoparticles (superparamagnetic iron-oxide, Fe₃O₄ or Fe₂O₃, Mn–Zn, and Fe–Au nanoparticles) are created and surface-modified using aminosilane, antibodies, PEG-phospholipids, or cyclic tripeptide of arginine-glycine-aspartic acid for the treatment of glioblastoma multiforme tumors [267–271]; or in the activation of reactive oxygen species via the p53

pathway in killing HepG2 human hepatocellular carcinoma and A549 human lung adenocarcinoma cells [272].

5.3.2. Antibacterial Activity

Since their discovery, antibiotics have been used in the treatment of diseases caused by bacteria. Unfortunately, due to the broad use of various antibiotics, drug-resistant bacteria develop and quickly become a challenge for human health. Therefore, novel methods for bacterial treatment need to be identified. Recently many studies have shown that metallic nanomaterials possess antibacterial activity. For instance, gold, silver, copper titanium, and iron nanoparticles exhibit physicochemical properties and antibacterial effects that depend on their size, structure, shape, and surface modification. Au nanoparticles show antibacterial properties at 2 nm size and Ag nanoparticles offer higher antibacterial properties with triangle-shaped nanoplates compared to other shapes. The underlying mechanisms of bactericidal effects of nanoparticles are diverse; metal nanoparticles are proposed to hinder bacterial growth by affecting the bacterial cell surface, entering into bacterial cells and inducing reactive oxygen species (ROS), damaging DNA, proteins, or inhibiting enzyme activities [273–275].

Among the metals mentioned above, silver plays a dominant role due to its antibacterial effects. Further, alloy nanoparticles combining silver with other metals exhibit better antibacterial properties; for instance, Cu–Ag alloy nanoparticles show more effective antibacterial properties than pure Ag or Cu nanoparticles in a resistant *Escherichia coli* strain (DH5a) and *Staphylococcus aureus* strain (BB255) [276,277]. In an experiment showing the benefit of combining Ag, Pt and Au, with the support of an Au core, the strong NIR SPR response could be transferred to the Ag–Pt alloy shell, and the alloy material endowed extra light-enhanced effects in its properties including overcoming bacterial resistance [278]. Further, Ag was added to a Co–Cr alloy material in an implant to improve the antibacterial characteristics of the material [279]. In addition to Ag-based alloy nanomaterials, other metal alloy nanomaterials such as Cu–Pt overcame bacterial resistance based on their peroxidase-like activity that can catalyze H_2O_2 and generate hydroxyl radicals, and inhibit bacterial growth [280].

5.3.3. Potential Vaccine Adjuvant

In vaccination, adjuvants accelerate antigen-specific immune responses. Adjuvants are necessary for the development of robust immune responses. Novel adjuvants are expected to have characteristics like induction of immunization against weak antigens, production of broadening immune response against pathogens with antigenic drift, and nontoxicity [281]. Recently, nanoparticles have also shown their potential as novel vaccine adjuvants. While being a vaccine carrier, nanoparticles enhance immune responses induced by vaccines as well. The immune activation effect of metallic nanoparticles is influenced by their size, shape, structure, crystallinity, surface modification, and ligands [281,282]. For example, aluminum hydroxide nanoparticles (112 nm) show stronger vaccine adjuvant activity than microparticles (9 μm) [283]. In an in vivo experiment performed in mice, gold nanoparticles coated with West Nile virus envelop protein induced a stronger antibody response with the 40 nm sphere shape than with the 20 nm sphere, cube, or rod-shaped nanoparticles [284].

Until now, only monometallic nanoparticles based on aluminum, gold mesoporous silica, iron, and nickel have been utilized as vaccine adjuvants. The use of bimetallic alloy nanoparticles in medical applications remains to be explored in future studies.

6. Conclusions and Future Perspectives

The above discussions provide compelling evidence that bimetallic or trimetallic alloy nanoparticles are more advantageous than monometallic nanoparticles in many fields because of their enhanced properties. The synergistic effect which arises from the combination of two or three metals contributes to these properties. This special characteristic creates multifunctional alloy nanoparticles that can be applied in various fields. Alloy nanoparticles also show other potential abilities. Using nanoparticles

with antibacterial activity to inhibit antibiotic-resistant bacteria is a topic for prospective studies. The role of nanoparticles as vaccine adjuvants is still in the early stages of research. Thus, an improvement in their existing properties promises superior advantages of using alloy nanoparticles in the future.

Author Contributions: Conceptualization, B.-H.J., S.H.L. and K.-H.H.; validation, H.C. and W.-Y.R.; writing, K.-H.H., X.-H.P. and J.K.; supervision, B.-H.J. All authors have read and agreed to the published version of the manuscript.

Funding: This research was funded by Konkuk University, 2018.

Acknowledgments: We acknowledge the Department of Bioscience and Biotechnology, Konkuk University, South Korea for support.

Conflicts of Interest: The authors declare no conflict of interest.

References

1. Ferrando, R.; Jellinek, J.; Johnston, R.L. Nanoalloys: From Theory to Applications of Alloy Clusters and Nanoparticles. *Chem. Rev.* **2008**, *108*, 845–910. [[CrossRef](#)] [[PubMed](#)]
2. Srinoi, P.; Chen, Y.-T.; Vittur, V.; Marquez, M.D.; Lee, T.R. Bimetallic Nanoparticles: Enhanced Magnetic and Optical Properties for Emerging Biological Applications. *Appl. Sci.* **2018**, *8*, 1106. [[CrossRef](#)]
3. Thota, S.; Wang, Y.; Zhao, J. Colloidal Au–Cu alloy nanoparticles: Synthesis, optical properties and applications. *Mater. Chem. Front.* **2018**, *2*, 1074–1089. [[CrossRef](#)]
4. Langlois, C.; Li, Z.; Yuan, J.; Alloyeau, D.; Nelayah, J.; Boichichio, D.; Ferrando, R.; Ricolleau, C. Transition from core–shell to Janus chemical configuration for bimetallic nanoparticles. *Nanoscale* **2012**, *4*, 3381. [[CrossRef](#)] [[PubMed](#)]
5. Nelli, D.; Krishnadas, A.; Ferrando, R.; Minnai, C. One-Step Growth of Core–Shell (PtPd)@Pt and (PtPd)@Pd Nanoparticles in the Gas Phase. *J. Phys. Chem. C* **2020**, *124*, 14338–14349. [[CrossRef](#)]
6. Ferrando, R. Symmetry breaking and morphological instabilities in core-shell metallic nanoparticles. *J. Physics Condens. Matter* **2015**, *27*, 013003. [[CrossRef](#)]
7. Baletto, F.; Mottet, C.; Ferrando, R. Growth of Three-Shell Onionlike Bimetallic Nanoparticles. *Phys. Rev. Lett.* **2003**, *90*, 135504. [[CrossRef](#)]
8. Ferrer, D.; Castro, A.T.; Gao, X.; Sepulveda-Guzman, S.; Ortiz-Méndez, U.; Jose-Yacamán, M. Three-Layer Core/Shell Structure in Au–Pd Bimetallic Nanoparticles. *Nano Lett.* **2007**, *7*, 1701–1705. [[CrossRef](#)]
9. Liu, R.; Priestley, R.D. Rational design and fabrication of core–shell nanoparticles through a one-step/pot strategy. *J. Mater. Chem. A* **2016**, *4*, 6680–6692. [[CrossRef](#)]
10. Liu, X.; Du, J.; Shao, Y.; Zhao, S.-F.; Yao, K.F. One-pot preparation of nanoporous Ag–Cu@Ag core-shell alloy with enhanced oxidative stability and robust antibacterial activity. *Sci. Rep.* **2017**, *7*, 10249. [[CrossRef](#)]
11. Purbia, R.; Paria, S. Yolk/shell nanoparticles: Classifications, synthesis, properties, and applications. *Nanoscale* **2015**, *7*, 19789–19873. [[CrossRef](#)]
12. Yec, C.C.; Zeng, H.C. Synthetic Architecture of Multiple Core–Shell and Yolk–Shell Structures of (Cu₂O)_nCu₂O (n = 1–4) with Centricity and Eccentricity. *Chem. Mater.* **2012**, *24*, 1917–1929. [[CrossRef](#)]
13. Basavegowda, N.; Mishra, K.; Lee, Y.R. Trimetallic FeAgPt alloy as a nanocatalyst for the reduction of 4-nitroaniline and decolorization of rhodamine B: A comparative study. *J. Alloy. Compd.* **2017**, *701*, 456–464. [[CrossRef](#)]
14. Bhunia, K.; Khilari, S.; Pradhan, D. Trimetallic PtAuNi alloy nanoparticles as an efficient electrocatalyst for the methanol electrooxidation reaction. *Dalton Trans.* **2017**, *46*, 15558–15566. [[CrossRef](#)] [[PubMed](#)]
15. Fang, B.; Wanjala, B.N.; Yin, J.; Loukrakpam, R.; Luo, J.; Hu, X.; Last, J.; Zhong, C.-J. Electrocatalytic performance of Pt-based trimetallic alloy nanoparticle catalysts in proton exchange membrane fuel cells. *Int. J. Hydrogen Energy* **2012**, *37*, 4627–4632. [[CrossRef](#)]
16. Gholivand, M.B.; Jalalvand, A.R.; Goicoechea, H.C.; Paimard, G.; Skov, T. Surface exploration of a room-temperature ionic liquid-chitin composite film decorated with electrochemically deposited PdFeNi trimetallic alloy nanoparticles by pattern recognition: An elegant approach to developing a novel biotin biosensor. *Talanta* **2015**, *131*, 249–258. [[CrossRef](#)]

17. Kang, S.W.; Lee, Y.W.; Park, Y.; Choi, B.-S.; Hong, J.W.; Park, K.-H.; Han, S.W. One-Pot Synthesis of Trimetallic Au@PdPt Core–Shell Nanoparticles with High Catalytic Performance. *ACS Nano* **2013**, *7*, 7945–7955. [[CrossRef](#)] [[PubMed](#)]
18. Karthikeyan, B.; Loganathan, B. Strategic green synthesis and characterization of Au/Pt/Ag trimetallic nanocomposites. *Mater. Lett.* **2012**, *85*, 53–56. [[CrossRef](#)]
19. Li, B.; Chan, S.H. PtFeNi tri-metallic alloy nanoparticles as electrocatalyst for oxygen reduction reaction in proton exchange membrane fuel cells with ultra-low Pt loading. *Int. J. Hydrogen Energy* **2013**, *38*, 3338–3345. [[CrossRef](#)]
20. Luo, J.; Wang, L.; Mott, D.; Njoki, P.N.; Kariuki, N.; Zhong, C.-J.; He, T. Ternary alloy nanoparticles with controllable sizes and composition and electrocatalytic activity. *J. Mater. Chem.* **2006**, *16*, 1665–1673. [[CrossRef](#)]
21. Richards, R.M. Introduction to nanoscale materials in chemistry, Edition II. In *Nanoscale Materials in Chemistry*, 2nd ed.; Klabunde, K.J., Richards, R.M., Eds.; John Wiley Sons Inc: Hoboken, NJ, USA, 2009; p. 804.
22. Panda, H. New Small Scale Ideas for Nanotechnology Industry. In *Nanoscience and Nanotechnology Handbook*; ASIA PACIFIC BUSINESS PRESS Inc: New Delhi, India, 2010.
23. Joshi, K.U.; Kabiraj, D.; Narsale, A.; Avasthi, D.; Warang, T.; Kothari, D. Embedded SiGe nanoparticles formed by atom beam co-sputtering of Si, Ge, SiO₂. *Surf. Coatings Technol.* **2009**, *203*, 2482–2485. [[CrossRef](#)]
24. Pannu, C.; Bala, M.; Khan, S.A.; Srivastava, S.K.; Kabiraj, D.; Avasthi, D. Synthesis and characterization of Au–Fe alloy nanoparticles embedded in a silica matrix by atom beam sputtering. *RSC Adv.* **2015**, *5*, 92080–92088. [[CrossRef](#)]
25. Naseri, N.; Sangpour, P.; Mousavi, S.H. Applying alloyed metal nanoparticles to enhance solar assisted water splitting. *RSC Adv.* **2014**, *4*, 46697–46703. [[CrossRef](#)]
26. Park, K.-W.; Sung, Y.-E.; Toney, M.F. Structural effect of PtRu–WO₃ alloy nanostructures on methanol electrooxidation. *Electrochem. Commun.* **2006**, *8*, 359–363. [[CrossRef](#)]
27. Sangpour, P.; Akhavan, O.; Moshfegh, A. rf reactive co-sputtered Au–Ag alloy nanoparticles in SiO₂ thin films. *Appl. Surf. Sci.* **2007**, *253*, 7438–7442. [[CrossRef](#)]
28. Sangpour, P.; Akhavan, O.; Moshfegh, A. The effect of Au/Ag ratios on surface composition and optical properties of co-sputtered alloy nanoparticles in Au–Ag:SiO₂ thin films. *J. Alloy. Compd.* **2009**, *486*, 22–28. [[CrossRef](#)]
29. Juhasz, J.A.; Best, S.M. Surface Modification of Biomaterials. In *6-Surface Modification of Biomaterials by Calcium Phosphate Deposition*; Williams, R., Ed.; Woodhead Publishing: Cambridge, UK, 2011; pp. 143–169.
30. Sharma, G.; Kumar, A.; Sharma, S.; Naushad, M.; Dwivedi, R.P.; Alothman, Z.A.; Mola, G.T. Novel development of nanoparticles to bimetallic nanoparticles and their composites: A review. *J. King Saud. Univ. Sci.* **2019**, *31*, 257–269. [[CrossRef](#)]
31. Gilroy, K.D.; Ruditskiy, A.; Peng, H.-C.; Qin, N.; Xia, Y. Bimetallic Nanocrystals: Syntheses, Properties, and Applications. *Chem. Rev.* **2016**, *116*, 10414–10472. [[CrossRef](#)]
32. Li, J.; Wu, Q.; Wu, J. Synthesis of Nanoparticles via Solvothermal and Hydrothermal Methods. In *Handbook of Nanoparticles*; Aliofkhazraei, M., Ed.; Springer International Publishing: Cham, Switzerland, 2016; pp. 295–328. [[CrossRef](#)]
33. Sharma, G.; Kumar, D.; Kumar, A.; Al-Muhtaseb, A.H.; Pathania, D.; Naushad, M.; Mola, G.T. Revolution from monometallic to trimetallic nanoparticle composites, various synthesis methods and their applications: A review. *Mater. Sci. Eng. C* **2017**, *71*, 1216–1230. [[CrossRef](#)]
34. An, L.; Yu, Y.; Li, X.; Liu, W.; Yang, H.; Wu, N.; Yang, S. Dextran-coated superparamagnetic amorphous Fe–Co nanoalloy for magnetic resonance imaging applications. *Mater. Res. Bull.* **2014**, *49*, 285–290. [[CrossRef](#)]
35. Cui, B.Z.; Marinescu, M.; Liu, J.F. High magnetization Fe–Co and Fe–Ni submicron and nanosize particles by thermal decomposition and hydrogen reduction. *J. Appl. Phys.* **2014**, *115*, 17A315. [[CrossRef](#)]
36. Huang, R.; Shao, G.-F.; Wen, Y.-H.; Sun, S.-G. Tunable thermodynamic stability of Au–CuPt core–shell trimetallic nanoparticles by controlling the alloy composition: Insights from atomistic simulations. *Phys. Chem. Chem. Phys.* **2014**, *16*, 22754–22761. [[CrossRef](#)]
37. Liu, Y.; Chi, Y.; Shan, S.; Yin, J.; Luo, J.; Zhong, C.-J. Characterization of magnetic NiFe nanoparticles with controlled bimetallic composition. *J. Alloy. Compd.* **2014**, *587*, 260–266. [[CrossRef](#)]

38. Lobiak, E.V.; Shlyakhova, E.; Bulusheva, L.; Plyusnin, P.E.; Shubin, Y.V.; Okotrub, A. Ni–Mo and Co–Mo alloy nanoparticles for catalytic chemical vapor deposition synthesis of carbon nanotubes. *J. Alloy. Compd.* **2015**, *621*, 351–356. [[CrossRef](#)]
39. Roshanghias, A.; Bernardi, J.; Ipser, H. An attempt to synthesize Sn–Zn–Cu alloy nanoparticles. *Mater. Lett.* **2016**, *178*, 10–14. [[CrossRef](#)]
40. Shevchenko, E.V.; Talapin, D.V.; Schnablegger, H.; Kornowski, A.; Festin, O.; Svedlindh, P.; Haase, M.; Weller, H. Study of Nucleation and Growth in the Organometallic Synthesis of Magnetic Alloy Nanocrystals: The Role of Nucleation Rate in Size Control of CoPt₃ Nanocrystals. *J. Am. Chem. Soc.* **2003**, *34*, 9090–9101. [[CrossRef](#)]
41. Vasquez, Y.; Luo, Z.; Schaak, R.E. Low-Temperature Solution Synthesis of the Non-Equilibrium Ordered Intermetallic Compounds Au₃Fe, Au₃Co, and Au₃Ni as Nanocrystals. *J. Am. Chem. Soc.* **2008**, *130*, 11866–11867. [[CrossRef](#)]
42. Xiao, S.; Hu, W.; Luo, W.; Wu, Y.; Li, X.; Deng, H. Size effect on alloying ability and phase stability of immiscible bimetallic nanoparticles. *Eur. Phys. J. B* **2006**, *54*, 479–484. [[CrossRef](#)]
43. Yin, S.; Li, Z.; Cheng, L.; Wang, C.; Liu, Y.; Chen, Q.; Gong, H.; Guo, L.; Li, Y.; Liu, Z. Magnetic PEGylated Pt₃Co nanoparticles as a novel MR contrast agent: In vivo MR imaging and long-term toxicity study. *Nanoscale* **2013**, *5*, 12464–12473. [[CrossRef](#)]
44. Bhunia, K.; Khilari, S.; Pradhan, D. Monodispersed PtPdNi Trimetallic Nanoparticles-Integrated Reduced Graphene Oxide Hybrid Platform for Direct Alcohol Fuel Cell. *ACS Sustain. Chem. Eng.* **2018**, *6*, 7769–7778. [[CrossRef](#)]
45. Călinescu, I.; Martin, D.; Ighigeanu, D.; Gavrilă, A.I.; Trifan, A.; Patrascu, M.; Munteanu, C.; Diacon, A.; Mănăilă, E.; Crăciun, G. Nanoparticles synthesis by electron beam radiolysis. *Open Chem.* **2014**, *12*, 774–781. [[CrossRef](#)]
46. Redjala, T.; Remita, H.; Apostolescu, G.; Mostafavi, M.; Thomazeau, C.; Uzio, D. Bimetallic Au–Pd and Ag–Pd Clusters Synthesised by γ or Electron Beam Radiolysis and Study of the Reactivity/Structure Relationships in the Selective Hydrogenation of Buta-1,3-Diene. *Oil Gas Sci. Technol. Rev. de l'IFP* **2006**, *61*, 789–797. [[CrossRef](#)]
47. Remita, H.; Etcheberry, A.; Belloni, J. Dose Rate Effect on Bimetallic Gold–Palladium Cluster Structure. *J. Phys. Chem. B* **2003**, *107*, 31–36. [[CrossRef](#)]
48. Tréguer, M.; De Cointet, C.; Remita, H.; Khatouri, J.; Mostafavi, M.; Amblard, J.; Belloni, J.; De Keyser, R. Dose Rate Effects on Radiolytic Synthesis of Gold–Silver Bimetallic Clusters in Solution. *J. Phys. Chem. B* **1998**, *102*, 4310–4321. [[CrossRef](#)]
49. Amendola, V.; Meneghetti, M.; Bakr, O.M.; Riello, P.; Polizzi, S.; Anjum, D.H.; Fiameni, S.; Arosio, P.; Orlando, T.; Fernández, C.D.J.; et al. Coexistence of plasmonic and magnetic properties in Au₈₉Fe₁₁ nanoalloys. *Nanoscale* **2013**, *5*, 5611–5619. [[CrossRef](#)] [[PubMed](#)]
50. Amendola, V.; Scaramuzza, S.; Littl, L.; Meneghetti, M.; Zuccolotto, G.; Rosato, A.; Nicolato, E.; Marzola, P.; Fracasso, G.; Anselmi, C.; et al. Magneto-Plasmonic Au–Fe Alloy Nanoparticles Designed for Multimodal SERS-MRI-CT Imaging. *Small* **2014**, *10*, 2476–2486. [[CrossRef](#)]
51. Swiatkowska-Warkocka, Z.; Koga, K.; Kawaguchi, K.; Wang, H.; Pyatenko, A.; Koshizaki, N. Pulsed laser irradiation of colloidal nanoparticles: A new synthesis route for the production of non-equilibrium bimetallic alloy submicrometer spheres. *RSC Adv.* **2013**, *3*, 79–83. [[CrossRef](#)]
52. Kugai, J.; Moriya, T.; Seino, S.; Nakagawa, T.; Ohkubo, Y.; Nitani, H.; Daimon, H.; Yamamoto, T.A. CeO₂-supported Pt–Cu alloy nanoparticles synthesized by radiolytic process for highly selective CO oxidation. *Int. J. Hydrogen Energy* **2012**, *37*, 4787–4797. [[CrossRef](#)]
53. Kuladeep, R.; Jyothi, L.; Alee, K.S.; Deepak, K.L.N.; Rao, D.N. Laser-assisted synthesis of Au–Ag alloy nanoparticles with tunable surface plasmon resonance frequency. *Opt. Mater. Express* **2012**, *2*, 161. [[CrossRef](#)]
54. Mirdamadi-Esfahani, M.; Mostafavi, M.; Keita, B.; Nadjo, L.; Kooyman, P.; Remita, H. Bimetallic Au–Pt nanoparticles synthesized by radiolysis: Application in electro-catalysis. *Gold Bull.* **2010**, *43*, 49–56. [[CrossRef](#)]
55. Oh, S.-D.; Kim, M.-R.; Choi, S.-H.; Chun, J.-H.; Lee, K.-P.; Gopalan, A.; Hwang, C.-G.; Sang-Ho, K.; Hoon, O.J. Radiolytic synthesis of Pd–M (M=Ag, Au, Cu, Ni and Pt) alloy nanoparticles and their use in reduction of 4-nitrophenol. *J. Ind. Eng. Chem.* **2008**, *14*, 687–692. [[CrossRef](#)]
56. Sarker, M.S.I.; Nakamura, T.; Herbani, Y.; Sato, S. Fabrication of Rh based solid-solution bimetallic alloy nanoparticles with fully-tunable composition through femtosecond laser irradiation in aqueous solution. *Appl. Phys. A* **2012**, *110*, 145–152. [[CrossRef](#)]

57. Yamamoto, T.A.; Nakagawa, T.; Seino, S.; Nitani, H. Bimetallic nanoparticles of PtM (M=Au, Cu, Ni) supported on iron oxide: Radiolytic synthesis and CO oxidation catalysis. *Appl. Catal. A Gen.* **2010**, *387*, 195–202. [[CrossRef](#)]
58. Sen, B.; Demirkan, B.; Şavk, A.; Gülbay, S.K.; Sen, F. Trimetallic PdRuNi nanocomposites decorated on graphene oxide: A superior catalyst for the hydrogen evolution reaction. *Int. J. Hydrogen Energy* **2018**, *43*, 17984–17992. [[CrossRef](#)]
59. Sharma, G.; Kumar, A.; Sharma, S.; Naushad, M.; Ahamad, T.; Al-Saeedi, S.I.; Al-Senani, G.M.; Al-Kadhi, N.S.; Stadler, F.J. Facile fabrication of Zr₂Ni₁Cu₇ trimetallic nano-alloy and its composite with Si₃N₄ for visible light assisted photodegradation of methylene blue. *J. Mol. Liq.* **2018**, *272*, 170–179. [[CrossRef](#)]
60. Sim, K.-S.; Jeon, J.-U.; Kwen, H.-D.; Choi, S.-H. Radiolytic Preparation of MWNT-Supported Electrocatalysts with Monometallic (Pt), Bimetallic (Pt-Ru), Trimetallic (Pt-Ru-Sn and Pt-Ru-Mo), and Tetrametallic (Pt-Ru-Mo-Sn) Nanoparticles for Direct Methanol Fuel Cells. *J. Nanoelectron. Optoelectron.* **2011**, *6*, 277–282. [[CrossRef](#)]
61. Yadav, N.; Jaiswal, A.K.; Dey, K.K.; Yadav, V.B.; Nath, G.; Srivastava, A.K.; Yadav, R.R. Trimetallic Au/Pt/Ag based nanofluid for enhanced antibacterial response. *Mater. Chem. Phys.* **2018**, *218*, 10–17. [[CrossRef](#)]
62. Fujimoto, T.; Terauchi, S.-Y.; Umehara, H.; Kojima, I.; Henderson, W. Sonochemical Preparation of Single-Dispersion Metal Nanoparticles from Metal Salts. *Chem. Mater.* **2001**, *13*, 1057–1060. [[CrossRef](#)]
63. Wang, R.; Hughes, T.; Beck, S.; Vakil, S.; Li, S.; Pantano, P.; Draper, R.K. Generation of toxic degradation products by sonication of Pluronic[®] dispersants: Implications for nanotoxicity testing. *Nanotoxicology* **2012**, *7*, 1272–1281. [[CrossRef](#)]
64. Xu, H.; Zeiger, B.; Suslick, K.S. Sonochemical synthesis of nanomaterials. *Chem. Soc. Rev.* **2013**, *42*, 2555–2567. [[CrossRef](#)]
65. Patil, A.B.; Bhanage, B.M. Sonochemistry: A Greener Protocol for Nanoparticles Synthesis. In *Handbook of Nanoparticles*; Aliofkhaezraei, M., Ed.; Springer International Publishing: Cham, Switzerland, 2016; pp. 143–166.
66. Mizukoshi, Y.; Okitsu, K.; Maeda, Y.; Yamamoto, T.A.; Oshima, R.; Nagata, Y. Sonochemical Preparation of Bimetallic Nanoparticles of Gold/Palladium in Aqueous Solution. *J. Phys. Chem. B* **1997**, *101*, 7033–7037. [[CrossRef](#)]
67. Okitsu, K.; Murakami, M.; Tanabe, S.; Matsumoto, H. Catalytic Behavior of Au Core/Pd Shell Bimetallic Nanoparticles on Silica. Prepared by Sonochemical and Sol-Gel Processes. *Chem. Lett.* **2000**, *29*, 1336–1337. [[CrossRef](#)]
68. Ono, Y.; Sekiguchi, K.; Sankoda, K.; Nii, S.; Namiki, N. Improved ultrasonic degradation of hydrophilic and hydrophobic aldehydes in water by combined use of atomization and UV irradiation onto the mist surface. *Ultrason. Sonochem.* **2019**, *60*, 104766. [[CrossRef](#)] [[PubMed](#)]
69. Anandan, S.; Grieser, F.; AshokKumar, M. Sonochemical Synthesis of Au–Ag Core–Shell Bimetallic Nanoparticles. *J. Phys. Chem. C* **2008**, *112*, 15102–15105. [[CrossRef](#)]
70. Gumeci, C.; Ua Cearnaigh, D.; Casadonte, D.J.; Korzeniewski, C. Synthesis of PtCu₃ bimetallic nanoparticles as oxygen reduction catalysts via a sonochemical method. *J. Mater. Chem. A* **2013**, *1*, 2322. [[CrossRef](#)]
71. Harika, V.K.; Sadhanala, H.K.; Perelshtein, I.; Gedanken, A. Sonication-Assisted Synthesis of Bimetallic Hg/Pd Alloy Nanoparticles for Catalytic Reduction of Nitrophenol and its Derivatives. *Ultrason. Sonochem.* **2019**, *60*, 104804. [[CrossRef](#)]
72. Jia, Y.; Niu, H.; Wu, M.; Ning, M.; Zhu, H.; Chen, Q. Sonochemical preparation of bimetallic Co/Cu nanoparticles in aqueous solution. *Mater. Res. Bull.* **2005**, *40*, 1623–1629. [[CrossRef](#)]
73. Matin, A.; Jang, J.-H.; Kwonad, Y.-U. One-pot sonication-assisted polyol synthesis of trimetallic core–shell (Pd,Co)@Pt nanoparticles for enhanced electrocatalysis. *Int. J. Hydrogen Energy* **2014**, *39*, 3710–3718. [[CrossRef](#)]
74. Mizukoshi, Y.; Fujimoto, T.; Nagata, Y.; Oshima, R.; Maeda, Y. Characterization and Catalytic Activity of Core–Shell Structured Gold/Palladium Bimetallic Nanoparticles Synthesized by the Sonochemical Method. *J. Phys. Chem. B* **2000**, *104*, 6028–6032. [[CrossRef](#)]
75. Wang, J.; Loh, K.P.; Zhong, Y.L.; Lin, M.; Ding, J.; Foo, Y.L. Bifunctional FePt Core–Shell and Hollow Spheres: Sonochemical Preparation and Self-Assembly. *Chem. Mater.* **2007**, *19*, 2566–2572. [[CrossRef](#)]
76. Burda, C.; Chen, X.; Narayanan, R.; El-Sayed, M.A. Chemistry and Properties of Nanocrystals of Different Shapes. *Chem. Rev.* **2005**, *105*, 1025–1102. [[CrossRef](#)]

77. Skrabalak, S.E.; Chen, J.; Sun, Y.; Lu, X.; Au, L.; Copley, C.M.; Xia, Y.; Copley, L.M. Gold Nanocages: Synthesis, Properties, and Applications. *Accounts Chem. Res.* **2008**, *41*, 1587–1595. [[CrossRef](#)]
78. Kumar-Krishnan, S.; Prokhorov, E.; Bahena, D.; Esparza, R.; Meyyappan, M. Chitosan-Covered Pd@Pt Core-Shell Nanocubes for Direct Electron Transfer in Electrochemical Enzymatic Glucose Biosensor. *ACS Omega* **2017**, *2*, 1896–1904. [[CrossRef](#)] [[PubMed](#)]
79. Nath, S.; Jana, S.; Pradhan, M.; Pal, T. Ligand-stabilized metal nanoparticles in organic solvent. *J. Colloid Interface Sci.* **2010**, *341*, 333–352. [[CrossRef](#)]
80. Selvakannan, P.; Sastry, M. Hollow gold and platinum nanoparticles by a transmetallation reaction in an organic solution. *Chem. Commun.* **2005**, 1684. [[CrossRef](#)] [[PubMed](#)]
81. Yang, J.; Lee, J.Y.; Too, H.-P. Core-Shell Ag-Au Nanoparticles from Replacement Reaction in Organic Medium. *J. Phys. Chem. B* **2005**, *109*, 19208–19212. [[CrossRef](#)] [[PubMed](#)]
82. Chen, J.; Wiley, B.J.; McLellan, J.; Xiong, Y.; Li, Z.-Y.; Xia, Y. Optical Properties of Pd-Ag and Pt-Ag Nanoboxes Synthesized via Galvanic Replacement Reactions. *Nano Lett.* **2005**, *5*, 2058–2062. [[CrossRef](#)] [[PubMed](#)]
83. Gao, J.; Ren, X.; Chen, N.; Tang, F.; Ren, J. Bimetallic Ag-Pt hollow nanoparticles: Synthesis and tunable surface plasmon resonance. *Scr. Mater.* **2007**, *57*, 687–690. [[CrossRef](#)]
84. Holewinski, A.; Idrobo, J.-C.; Linic, S. High-performance Ag-Co alloy catalysts for electrochemical oxygen reduction. *Nat. Chem.* **2014**, *6*, 828–834. [[CrossRef](#)] [[PubMed](#)]
85. Li, H.; Wu, H.; Zhai, Y.; Xu, X.; Jin, Y. Synthesis of Monodisperse Plasmonic Au Core-Pt Shell Concave Nanocubes with Superior Catalytic and Electrocatalytic Activity. *ACS Catal.* **2013**, *3*, 2045–2051. [[CrossRef](#)]
86. Liu, X.; Fu, G.; Chen, Y.; Tang, Y.; She, P.; Lu, T. Pt-Pd-Co Trimetallic Alloy Network Nanostructures with Superior Electrocatalytic Activity towards the Oxygen Reduction Reaction. *Chem. A Eur. J.* **2013**, *20*, 585–590. [[CrossRef](#)]
87. Singh, S.; Srivastava, P.; Singh, G. Synthesis, characterization of Co-Ni-Cu trimetallic alloy nanocrystals and their catalytic properties, Part – 91. *J. Alloy. Compd.* **2013**, *562*, 150–155. [[CrossRef](#)]
88. Wang, Z.-L.; Ping, Y.; Yan, J.-M.; Wang, H.; Jiang, Q. Hydrogen generation from formic acid decomposition at room temperature using a NiAuPd alloy nanocatalyst. *Int. J. Hydrogen Energy* **2014**, *39*, 4850–4856. [[CrossRef](#)]
89. Xu, Y.; Yuan, Y.; Ma, A.; Wu, X.; Liu, Y.; Zhang, B. Composition-Tunable Pt-Co Alloy Nanoparticle Networks: Facile Room-Temperature Synthesis and Supportless Electrocatalytic Applications. *ChemPhysChem* **2012**, *13*, 2601–2609. [[CrossRef](#)] [[PubMed](#)]
90. Zhang, J.; Chen, G.; Guay, D.; Chaker, M.; Ma, D. Highly active PtAu alloy nanoparticle catalysts for the reduction of 4-nitrophenol. *Nanoscale* **2014**, *6*, 2125–2130. [[CrossRef](#)]
91. Zhang, J.-M.; Wang, R.-X.; Nong, R.-J.; Li, Y.; Zhang, X.; Zhang, P.-Y.; Fan, Y.-J. Hydrogen co-reduction synthesis of PdPtNi alloy nanoparticles on carbon nanotubes as enhanced catalyst for formic acid electrooxidation. *Int. J. Hydrogen Energy* **2017**, *42*, 7226–7234. [[CrossRef](#)]
92. Zhou, S.; Jackson, G.S.; Eichhorn, B.W. AuPt Alloy Nanoparticles for CO-Tolerant Hydrogen Activation: Architectural Effects in Au-Pt Bimetallic Nanocatalysts. *Adv. Funct. Mater.* **2007**, *17*, 3099–3104. [[CrossRef](#)]
93. Da Silva, A.G.M.; Rodrigues, T.S.; Haigh, S.J.; Camargo, P.H.C. Galvanic replacement reaction: Recent developments for engineering metal nanostructures towards catalytic applications. *Chem. Commun.* **2017**, 53, 7135–7148. [[CrossRef](#)]
94. Lu, X.; Chen, J.; E Skrabalak, S.; Xia, Y. Galvanic replacement reaction: A simple and powerful route to hollow and porous metal nanostructures. *Proc. Inst. Mech. Eng. Part N J. Nanoeng. Nanosyst.* **2007**, *221*, 1–16. [[CrossRef](#)]
95. El Mel, A.-A.; Chettab, M.; Gautron, E.; Chauvin, A.; Humbert, B.; Mevellec, J.-Y.; Delacote, C.; Thiry, D.; Stephant, N.; Ding, J.; et al. Galvanic Replacement Reaction: A Route to Highly Ordered Bimetallic Nanotubes. *J. Phys. Chem. C* **2016**, *120*, 17652–17659. [[CrossRef](#)]
96. Pham, V.V.; Ta, V.-T.; Sunglae, C. Synthesis of NiPt alloy nanoparticles by galvanic replacement method for direct ethanol fuel cell. *Int. J. Hydrogen Energy* **2017**, *42*, 13192–13197. [[CrossRef](#)]
97. Liu, X.; Wang, A.; Li, L.; Zhang, T.; Mou, C.-Y.; Lee, J.-F. Synthesis of Au-Ag alloy nanoparticles supported on silica gel via galvanic replacement reaction. *Prog. Nat. Sci.* **2013**, *23*, 317–325. [[CrossRef](#)]
98. Zhang, Y.; Zhu, P.; Li, G.; Cui, Z.; Cui, C.; Zhang, K.; Gao, J.; Chen, X.; Zhang, G.; Sun, R.; et al. PVP-Mediated Galvanic Replacement Synthesis of Smart Elliptic Cu-Ag Nanoflakes for Electrically Conductive Pastes. *ACS Appl. Mater. Interfaces* **2019**, *11*, 8382–8390. [[CrossRef](#)] [[PubMed](#)]

99. Ustarroz, J.; Hubin, A.; Terryn, H. Supported Nanoparticle Synthesis by Electrochemical Deposition. In *Handbook of Nanoparticles*; Aliofkhaezrai, M., Ed.; Springer International Publishing: Cham, Switzerland, 2016; pp. 603–631.
100. Elemike, E.E.; Onwudiwe, D.C.; Fayemi, O.E.; Botha, T.L. Green synthesis and electrochemistry of Ag, Au, and Ag–Au bimetallic nanoparticles using golden rod (*Solidago canadensis*) leaf extract. *Appl. Phys. A* **2019**, *125*, 42. [[CrossRef](#)]
101. Gao, H.; Xiao, F.; Ching, C.B.; Duan, H. One-Step Electrochemical Synthesis of PtNi Nanoparticle-Graphene Nanocomposites for Nonenzymatic Amperometric Glucose Detection. *ACS Appl. Mater. Interfaces* **2011**, *3*, 3049–3057. [[CrossRef](#)]
102. Hung, N.D.; Van Cong, T.; Trang, H.N. Synthesis of bimetallic Cu-Ag nanoparticles prepared by DC high voltage electrochemical method. *Vietnam. J. Chem.* **2019**, *57*, 609–614. [[CrossRef](#)]
103. Li, D.; Liu, J.; Wang, H.; Barrow, C.J.; Yang, W. Electrochemical synthesis of fractal bimetallic Cu/Ag nanodendrites for efficient surface enhanced Raman spectroscopy. *Chem. Commun.* **2016**, *52*, 10968–10971. [[CrossRef](#)]
104. Mancier, V.; Rousse-Bertrand, C.; Dille, J.; Michel, J.; Fricoteaux, P. Sono and electrochemical synthesis and characterization of copper core–silver shell nanoparticles. *Ultrason. Sonochem.* **2010**, *17*, 690–696. [[CrossRef](#)]
105. Ostrom, C.K.; Chen, A. Synthesis and Electrochemical Study of Pd-Based Trimetallic Nanoparticles for Enhanced Hydrogen Storage. *J. Phys. Chem. C* **2013**, *117*, 20456–20464. [[CrossRef](#)]
106. Querejeta, A.; Del Barrio, M.; García, S. Electrochemical synthesis of Rh-Pd bimetallic nanoparticles onto a glassy carbon surface. *J. Electroanal. Chem.* **2016**, *778*, 98–102. [[CrossRef](#)]
107. Raof, J.B.; Ojani, R.; Rashid-Nadimi, S. Electrochemical synthesis of bimetallic Au@Pt nanoparticles supported on gold film electrode by means of self-assembled monolayer. *J. Electroanal. Chem.* **2010**, *641*, 71–77. [[CrossRef](#)]
108. Ren, H.-X.; Huang, X.-J.; Kim, J.-H.; Choi, Y.-K.; Gu, N. Pt/Au bimetallic hierarchical structure with micro/nano-array via photolithography and electrochemical synthesis: From design to GOT and GPT biosensors. *Talanta* **2009**, *78*, 1371–1377. [[CrossRef](#)] [[PubMed](#)]
109. Yancey, D.F.; Carino, E.V.; Crooks, R.M. Electrochemical Synthesis and Electrocatalytic Properties of Au@Pt Dendrimer-Encapsulated Nanoparticles. *J. Am. Chem. Soc.* **2010**, *132*, 10988–10989. [[CrossRef](#)] [[PubMed](#)]
110. Yang, C.Y. Electrochemical Synthesis of PtAu Bimetallic Nanoparticles on Multiwalled Carbon Nanotubes and Application for Amperometric Determination of Nitrite. *Int. J. Electrochem. Sci.* **2016**, *11*, 4027–4036. [[CrossRef](#)]
111. Yang, J.; Deng, S.; Lei, J.; Ju, H.; Gunasekaran, S. Electrochemical synthesis of reduced graphene sheet–AuPd alloy nanoparticle composites for enzymatic biosensing. *Biosens. Bioelectron.* **2011**, *29*, 159–166. [[CrossRef](#)] [[PubMed](#)]
112. Byrappa, K.; Yoshimura, M. Hydrothermal Technology—Principles and Applications. In *Handbook of Hydrothermal Technology*; William Andrew Inc: Norwich, NY, USA, 2001; pp. 1–52.
113. Gan, Y.X.; Jayatissa, A.H.; Yu, Z.; Chen, X.; Li, M. Hydrothermal Synthesis of Nanomaterials. *J. Nanomater.* **2020**, *2020*, 1–3. [[CrossRef](#)]
114. Rák, Z.; Brenner, D.W. Negative Surface Energies of Nickel Ferrite Nanoparticles under Hydrothermal Conditions. *J. Nanomater.* **2019**, *2019*, 1–6. [[CrossRef](#)]
115. Ma, L.; Wei, Z.; Zhu, X.; Liang, J.; Zhang, X. Synthesis and Photocatalytic Properties of Co-Doped Zn_{1-x}CoxMn₂O Hollow Nanospheres. *J. Nanomater.* **2019**. [[CrossRef](#)]
116. Saeed, G.H.M.; Radiman, S.; Gasaymeh, S.S.; Lim, H.N.; Huang, N.M. Mild Hydrothermal Synthesis of Ni–Cu Nanoparticles. *J. Nanomater.* **2010**, *2010*, 1–5. [[CrossRef](#)]
117. Yesmurzayeva, N.; Tursunova, R.; Nakypova, S.; Selenova, B.; Kudaibergenov, S. Synthesis and characterization of catalysts based on bimetallic nanoparticles. In Proceedings of the 2016 International Conference on Nanomaterials: Application & Properties (NAP), Lviv, Ukraine, 14–19 September 2016; Institute of Electrical and Electronics Engineers (IEEE): Piscataway, NJ, USA, 2016.
118. Liu, Y.; Shen, X. Preparation and characterization of NiFe bimetallic micro-particles and its composite with silica shell. *J. Saudi Chem. Soc.* **2019**, *23*, 1032–1040. [[CrossRef](#)]
119. Wang, B.; Huang, X.; Zhu, Z.; Huang, H.; Dai, J. Hydrothermal synthesis of cobalt–nickel bimetallic phosphides. *Appl. Nanosci.* **2012**, *2*, 481–485. [[CrossRef](#)]

120. Dahman, Y.; Deonanan, K.; Dontsos, T.; Iammatteo, A. Chapter 6 – Nanopolymers. In *Nanotechnology and Functional Materials for Engineers*; Dahman, Y., Ed.; Elsevier: Amsterdam, The Netherlands, 2017; pp. 121–144.
121. Ojovan, M.I.; Lee, W.E.; Kalmykov, S.N. Chapter 16 - Treatment of Radioactive Wastes. In *An Introduction to Nuclear Waste Immobilisation*, 3rd ed.; Ojovan, M.I., Lee, W.E., Kalmykov, S.N., Eds.; Elsevier: Amsterdam, The Netherlands, 2019; pp. 231–269.
122. Khan, S.R.; Batool, M.; Jamil, S.; Bibi, S.; Abid, S.; Janjua, M.R.S.A. Synthesis and Characterization of Mg–Zn Bimetallic Nanoparticles: Selective Hydrogenation of p-Nitrophenol, Degradation of Reactive Carbon Black 5 and Fuel Additive. *J. Inorg. Organomet. Polym. Mater.* **2019**, *30*, 438–450. [[CrossRef](#)]
123. Wang, X.; Chen, C.; Chang, Y.; Liu, H. Dechlorination of chlorinated methanes by Pd/Fe bimetallic nanoparticles. *J. Hazard. Mater.* **2009**, *161*, 815–823. [[CrossRef](#)]
124. Allaedini, G.; Tasirin, S.M.; Aminayi, P. Synthesis of Fe–Ni–Ce trimetallic catalyst nanoparticles via impregnation and co-precipitation and their application to dye degradation. *Chem. Pap.* **2016**, *70*, 231–242. [[CrossRef](#)]
125. Nunes, D.; Pimentel, A.; Santos, L.; Barquinha, P.; Pereira, L.; Fortunato, E.; Martins, R. Synthesis, design, and morphology of metal oxide nanostructures. In *Metal Oxide Nanostructures*; Nunes, D., Pimentel, A., Santos, L., Barquinha, P., Pereira, L., Fortunato, E., Martins, R., Eds.; Elsevier: Amsterdam, The Netherlands, 2019; pp. 21–57.
126. Pisduangdaw, S.; Panpranot, J.; Methastidsook, C.; Chaisuk, C.; Faungnawakij, K.; Praserttham, P.; Mekasuwandumrong, O. Characteristics and catalytic properties of Pt–Sn/Al₂O₃ nanoparticles synthesized by one-step flame spray pyrolysis in the dehydrogenation of propane. *Appl. Catal. A Gen.* **2009**, *370*, 1–6. [[CrossRef](#)]
127. Jung, J.-W.; Kim, W.-I.; Kim, J.-R.; Oh, K.; Koh, H.L. Effect of Direct Reduction Treatment on Pt–Sn/Al₂O₃ Catalyst for Propane Dehydrogenation. *Catalysts* **2019**, *9*, 446. [[CrossRef](#)]
128. Devarajan, S.; Bera, P.; Sampath, S. Bimetallic nanoparticles: A single step synthesis, stabilization, and characterization of Au–Ag, Au–Pd, and Au–Pt in sol–gel derived silicates. *J. Colloid Interface Sci.* **2005**, *290*, 117–129. [[CrossRef](#)] [[PubMed](#)]
129. Singh, L.P.; Bhattacharyya, S.K.; Kumar, R.; Mishra, G.; Sharma, U.; Singh, G.; Ahalawat, S. Sol-Gel processing of silica nanoparticles and their applications. *Adv. Colloid Interface Sci.* **2014**, *214*, 17–37. [[CrossRef](#)]
130. Suyal, G. Bimetallic colloids of silver and copper in thin films: Sol–gel synthesis and characterization. *Thin Solid Films* **2003**, *426*, 53–61. [[CrossRef](#)]
131. Golabiewska, A.; Lisowski, W.; Jarek, M.; Nowaczyk, G.; Michalska, M.; Jurga, S.; Zaleska-Medynska, A. The effect of metals content on the photocatalytic activity of TiO₂ modified by Pt/Au bimetallic nanoparticles prepared by sol-gel method. *Mol. Catal.* **2017**, *442*, 154–163. [[CrossRef](#)]
132. Pradhan, A.C.; Paul, A.; Rao, G.R. Sol-gel-cum-hydrothermal synthesis of mesoporous Co-Fe@Al₂O₃–MCM-41 for methylene blue remediation. *J. Chem. Sci.* **2017**, *129*, 381–395. [[CrossRef](#)]
133. Burger, M.J.; Robinson, B.J.; Pease, L.F. Sol-Gel-Derived Nanoscale Materials. In *Handbook of Nanoparticles*; Aliofkhaezraei, M., Ed.; Springer International Publishing: Cham, Switzerland, 2016; pp. 691–714.
134. Salmones, J.; Wang, J.-A.; A Galicia, J.; Aguilar, J.A.G. H₂ reduction behaviors and catalytic performance of bimetallic tin-modified platinum catalysts for propane dehydrogenation. *J. Mol. Catal. A Chem.* **2002**, *184*, 203–213. [[CrossRef](#)]
135. Zieliska-Jurek, A.; Reszczyska, J.; Grabowska, E.; Zaleska, A.; Zielińska-Jurek, J.R.A. Nanoparticles Preparation Using Microemulsion Systems. In *Microemulsions - An Introduction to Properties and Applications*; Najjar, R., Ed.; Croatia Intech: Rijeka, Croatia, 2012; pp. 229–250.
136. Malik, M.A.; Wani, M.Y.; Hashim, M.A. Microemulsion method: A novel route to synthesize organic and inorganic nanomaterials: 1st Nano Update. *Arab. J. Chem.* **2012**, *5*, 397–417. [[CrossRef](#)]
137. Tojo, C.; Blanco, M.C.; López-Quintela, M.A.; Rivas, R. Synthesis of Nanoparticles in Microemulsions: A comparison study between experimental and simulation results. In *Non-Crystalline and Nanoscale Materials, Proceedings of the Fifth International Workshop on Non-Crystalline Solids, Santiago de Compostela, Spain, 2–5 July 1997*; Rivas, R., Ed.; World Scientific Pub Co Pte Lt: London, UK, 1998; pp. 451–456.
138. Magno, L.M.; Sigle, W.; Van Aken, P.A.; Angelescu, D.G.; Stubenrauch, C. Microemulsions as Reaction Media for the Synthesis of Bimetallic Nanoparticles: Size and Composition of Particles. *Chem. Mater.* **2010**, *22*, 6263–6271. [[CrossRef](#)]

139. Wang, H.-K.; Yi, C.-Y.; Tian, L.; Wang, W.-J.; Fang, J.; Zhao, J.; Shen, W.-G. Ag-Cu Bimetallic Nanoparticles Prepared by Microemulsion Method as Catalyst for Epoxidation of Styrene. *J. Nanomater.* **2012**, *2012*, 1–8. [[CrossRef](#)]
140. Tojo, C.; De Dios, M.; Buceta, D.; Lopez-Quintela, M.A. Cage-like effect in Au–Pt nanoparticle synthesis in microemulsions: A simulation study. *Phys. Chem. Chem. Phys.* **2014**, *16*, 19720–19731. [[CrossRef](#)] [[PubMed](#)]
141. Abazari, R.; Heshmatpour, F.; Balalaie, S. Pt/Pd/Fe Trimetallic Nanoparticle Produced via Reverse Micelle Technique: Synthesis, Characterization, and Its Use as an Efficient Catalyst for Reductive Hydrodehalogenation of Aryl and Aliphatic Halides under Mild Conditions. *ACS Catal.* **2012**, *3*, 139–149. [[CrossRef](#)]
142. Zhang, X.; Zhang, F.; Guan, R.-F.; Chan, K.-Y. Preparation of Pt-Ru-Ni ternary nanoparticles by microemulsion and electrocatalytic activity for methanol oxidation. *Mater. Res. Bull.* **2007**, *42*, 327–333. [[CrossRef](#)]
143. Cantillo, N.M.; Solla-Gullón, J.; Herrero, E.; Sánchez, C. Ethanol Electrooxidation on PtSnNi/C Nanoparticles Prepared in Water-In-Oil Microemulsion. *ECS Trans.* **2011**, *41*, 1307–1316. [[CrossRef](#)]
144. Singh, P.; Kim, Y.-J.; Zhang, D.; Yang, D.-C. Biological Synthesis of Nanoparticles from Plants and Microorganisms. *Trends Biotechnol.* **2016**, *34*, 588–599. [[CrossRef](#)]
145. Karthik, L.; Kirthi, A.V.; Ranjan, S.; Srinivasan, V.M. Bacterial Synthesis of Nanoparticles and Their Applications. In *Biological Synthesis of Nanoparticles and Their Applications*, 1st ed.; Karthik, L., Kirthi, A.V., Ranjan, S., Srinivasan, V.M., Eds.; CRC Press: Boca Raton, FA, USA, 2020.
146. Raveendran, P.; Fu, J.; Wallen, S.L. Completely “Green” Synthesis and Stabilization of Metal Nanoparticles. *J. Am. Chem. Soc.* **2003**, *125*, 13940–13941. [[CrossRef](#)] [[PubMed](#)]
147. Xia, B.; He, F.; Li, L. Preparation of Bimetallic Nanoparticles Using a Facile Green Synthesis Method and Their Application. *Langmuir* **2013**, *29*, 4901–4907. [[CrossRef](#)] [[PubMed](#)]
148. Park, T.J.; Lee, K.G.; Lee, S.Y. Advances in microbial biosynthesis of metal nanoparticles. *Appl. Microbiol. Biotechnol.* **2015**, *100*, 521–534. [[CrossRef](#)]
149. Gahlawat, G.; Choudhury, A.R. A review on the biosynthesis of metal and metal salt nanoparticles by microbes. *RSC Adv.* **2019**, *9*, 12944–12967. [[CrossRef](#)]
150. Deplanche, K.; Merroun, M.L.; Casadesus, M.; Tran, D.T.; Mikheenko, I.P.; Bennett, J.A.; Zhu, J.; Jones, I.P.; Attard, G.A.; Wood, J.; et al. Microbial synthesis of core/shell gold/palladium nanoparticles for applications in green chemistry. *J. R. Soc. Interface* **2012**, *9*, 1705–1712. [[CrossRef](#)]
151. Gomez-Bolivar, J.; Mikheenko, I.P.; Orozco, R.L.; Sharma, S.; Banerjee, D.; Walker, M.; Hand, R.A.; Merroun, M.L.; Macaskie, L.E. Synthesis of Pd/Ru Bimetallic Nanoparticles by *Escherichia coli* and Potential as a Catalyst for Upgrading 5-Hydroxymethyl Furfural Into Liquid Fuel Precursors. *Front. Microbiol.* **2019**, *10*, 1276. [[CrossRef](#)]
152. Tuo, Y.; Liu, G.; Dong, B.; Yu, H.; Zhou, J.; Wang, J.; Jin, R. Microbial synthesis of bimetallic PdPt nanoparticles for catalytic reduction of 4-nitrophenol. *Environ. Sci. Pollut. Res.* **2017**, *24*, 5249–5258. [[CrossRef](#)]
153. Han, R.; Song, X.; Wang, Q.; Qi, Y.; Deng, G.; Zhang, A.; Wang, Q.; Chang, F.; Wu, C.; Cheng, Y. Microbial synthesis of graphene-supported highly-dispersed Pd-Ag bimetallic nanoparticles and its catalytic activity. *J. Chem. Technol. Biotechnol.* **2019**, *94*, 3375–3383. [[CrossRef](#)]
154. Jena, P.; Bhattacharya, M.; Bhattacharjee, G.; Satpati, B.; Mukherjee, P.; Senapati, D.; Srinivasan, R. Bimetallic gold–silver nanoparticles mediate bacterial killing by disrupting the actin cytoskeleton MreB. *Nanoscale* **2020**, *12*, 3731–3749. [[CrossRef](#)]
155. Tuo, Y.; Liu, G.; Dong, B.; Zhou, J.; Wang, A.; Wang, J.; Jin, R.; Lv, H.; Dou, Z.; Huang, W. Microbial synthesis of Pd/Fe₃O₄, Au/Fe₃O₄ and PdAu/Fe₃O₄ nanocomposites for catalytic reduction of nitroaromatic compounds. *Sci. Rep.* **2015**, *5*, 13515. [[CrossRef](#)]
156. De Corte, S.; Henebel, T.; Fitts, J.P.; Sabbe, T.; Bliznuk, V.; Verschuere, S.; Van Der Lelie, D.; Verstraete, W.; Boon, N. Biosupported Bimetallic Pd–Au Nanocatalysts for Dechlorination of Environmental Contaminants. *Environ. Sci. Technol.* **2011**, *45*, 8506–8513. [[CrossRef](#)]
157. Ghorbani, H.R.; Rashidi, R. Synthesis of Cu–Ag nanoparticles by biological method. *Inorg. Nano-Metal Chem.* **2017**, *48*, 41–43. [[CrossRef](#)]
158. Alghuthaymi, M.A.; Almoammar, H.; Rai, M.K.; Said-Galiev, E.; A Abd-Elsalam, K. Myconanoparticles: Synthesis and their role in phytopathogens management. *Biotechnol. Biotech. Eq.* **2015**, *29*, 221–236. [[CrossRef](#)] [[PubMed](#)]

159. Moghaddam, A.B.; Namvar, F.; Moniri, M.; Tahir, P.M.; Azizi, S.; Mohamad, R. Nanoparticles Biosynthesized by Fungi and Yeast: A Review of Their Preparation, Properties, and Medical Applications. *Molecules* **2015**, *20*, 16540–16565. [[CrossRef](#)] [[PubMed](#)]
160. Sawle, B.D.; Salimath, B.; Deshpande, R.; Bedre, M.D.; Prabhakar, B.K.; Venkataraman, A. Biosynthesis and stabilization of Au and Au-Ag alloy nanoparticles by fungus, *Fusarium semitectum*. *Sci. Technol. Adv. Mater.* **2008**, *9*, 035012. [[CrossRef](#)]
161. Senapati, S.; Ahmad, A.; Khan, M.I.; Sastry, M.; Kumar, R. Extracellular Biosynthesis of Bimetallic Au-Ag Alloy Nanoparticles. *Small* **2005**, *1*, 517–520. [[CrossRef](#)]
162. Castro-Longoria, E.; Vilchis-Nestor, A.R.; Avalos-Borja, M. Biosynthesis of silver, gold and bimetallic nanoparticles using the filamentous fungus *Neurospora crassa*. *Colloids Surfaces Biointerfaces* **2011**, *83*, 42–48. [[CrossRef](#)]
163. Ahmad, A.; Mukherjee, P.; Mandal, D.; Senapati, S.; Khan, M.I.; Kumar, R.; Sastry, M. Enzyme Mediated Extracellular Synthesis of CdS Nanoparticles by the Fungus, *Fusarium oxysporum*. *J. Am. Chem. Soc.* **2002**, *124*, 12108–12109. [[CrossRef](#)]
164. Reyes, L.R.; Gómez, I.; Garza, M.T. Biosynthesis of Cadmium Sulfide Nanoparticles by the Fungi *Fusarium* sp. *Int. J. Nanotechnol. Biomed.* **2009**, *1*, 90–95. [[CrossRef](#)]
165. Borovaya, M.; Pirko, Y.; Krupodorova, T.; Naumenko, A.; Blume, Y.; Yemets, A. Biosynthesis of cadmium sulphide quantum dots by using *Pleurotus ostreatus* (Jacq.) P. Kumm. *Biotechnol. Biotec. Eq.* **2015**, *29*, 1–8. [[CrossRef](#)]
166. Sanghi, R.; Verma, P. A facile green extracellular biosynthesis of CdS nanoparticles by immobilized fungus. *Chem. Eng. J.* **2009**, *155*, 886–891. [[CrossRef](#)]
167. Feng, H. Green Biosynthesis of CdS Nanoparticles Using Yeast Cells for Fluorescence Detection of Nucleic Acids and Electrochemical Detection of Hydrogen Peroxide. *Int. J. Electrochem. Sci.* **2017**, *12*, 618–628. [[CrossRef](#)]
168. Prasad, K.; Jha, A.K. Biosynthesis of CdS nanoparticles: An improved green and rapid procedure. *J. Colloid Interface Sci.* **2010**, *342*, 68–72. [[CrossRef](#)] [[PubMed](#)]
169. Kulkarni, S.K. Introduction to Quantum Mechanics. In *Nanotechnology: Principles and Practices*; Springer International Publishing: New Delhi, India, 2015; pp. 1–29.
170. Krumov, N.; Oder, S.; Perner-Nochta, I.; Angelov, A.; Posten, C. Accumulation of CdS nanoparticles by yeasts in a fed-batch bioprocess. *J. Biotechnol.* **2007**, *132*, 481–486. [[CrossRef](#)]
171. Love, A.J.; Makarov, V.; Yaminsky, I.V.; Kalinina, N.O.; Taliany, M.E. The use of tobacco mosaic virus and cowpea mosaic virus for the production of novel metal nanomaterials. *Virology* **2014**, *449*, 133–139. [[CrossRef](#)]
172. Banik, S.; Sharma, P. Plant pathology in the era of nanotechnology. *Indian Phytopathol.* **2011**, *64*, 120–127.
173. Young, M.; Debbie, W.; Uchida, M.; Douglas, T. Plant Viruses as Biotemplates for Materials and Their Use in Nanotechnology. *Annu. Rev. Phytopathol.* **2008**, *46*, 361–384. [[CrossRef](#)]
174. Shah, S.N.; Steinmetz, N.F.; Aljabali, A.A.A.; Lomonosoff, G.P.; Evans, D.J. Environmentally benign synthesis of virus-templated, monodisperse, iron-platinum nanoparticles. *Dalton Trans.* **2009**, 8479. [[CrossRef](#)]
175. Tsukamoto, R.; Muraoka, M.; Seki, M.; Tabata, H.; Yamashita, I. Synthesis of CoPt and FePt₃Nanowires Using the Central Channel of Tobacco Mosaic Virus as a Biotemplate. *Chem. Mater.* **2007**, *19*, 2389–2391. [[CrossRef](#)]
176. Loo, L.; Guenther, R.H.; Lommel, S.A.; Franzen, S. Encapsulation of Nanoparticles by Red Clover Necrotic Mosaic Virus. *J. Am. Chem. Soc.* **2007**, *129*, 11111–11117. [[CrossRef](#)]
177. Parihar, P.; Singh, S.; Singh, R.; Rajasheker, G.; Rathnagiri, P.; Srivastava, R.K.; Singh, V.P.; Suprasanna, P.; Prasad, S.M.; Kishor, P.K. An Integrated Transcriptomic, Proteomic, Metabolomic Approach to Unravel the Molecular Mechanisms of Metal Stress Tolerance in Plants. In *Plant-Metal Interactions*; Srivastava, S., Srivastava, A.K., Suprasanna, P., Eds.; Springer International Publishing: Cham, Switzerland, 2019.
178. Pal, G.; Rai, P.; Pandey, A. Green synthesis of nanoparticles: A greener approach for a cleaner future. In *Green Synthesis, Characterization and Applications of Nanoparticles*; Shukla, A.K., Iravani, S., Eds.; Elsevier: Amsterdam, The Netherlands; 548, pp. 1–26.
179. Akinsiku, A.A.; Dare, E.O.; Ajanaku, K.O.; Ajani, O.O.; Olugbuyiro, J.A.O.; Siyanbola, T.O.; Ejilude, O.; Emeteri, M.E. Modeling and Synthesis of Ag and Ag/Ni Allied Bimetallic Nanoparticles by Green Method: Optical and Biological Properties. *Int. J. Biomater.* **2018**, *2018*, 1–17. [[CrossRef](#)] [[PubMed](#)]

180. Akinsiku, A.A.; Dare, E.O.; Ajani, O.O.; Ayo-Ajayi, J.; Ademosun, O.T.; Ajayi, S.O. Room temperature Phytosynthesis of Ag/Co bimetallic nanoparticles using aqueous leaf extract of *Canna indica*. *IOP Conf. Ser. Earth Environ. Sci.* **2018**, *173*, 012019. [[CrossRef](#)]
181. Olajire, A.A.; Kareem, A.; Olaleke, A. Green synthesis of bimetallic Pt@Cu nanostructures for catalytic oxidative desulfurization of model oil. *J. Nanostructure Chem.* **2017**, *7*, 159–170. [[CrossRef](#)]
182. Zhang, G.; Du, M.; Li, Q.; Li, X.; Huang, J.; Jiang, X.; Sun, D. Green synthesis of Au–Ag alloy nanoparticles using *Cacumen platycladi* extract. *RSC Adv.* **2013**, *3*, 1878–1884. [[CrossRef](#)]
183. Mohamad, N.A.N.; Arham, N.; Junaidah, J.; Hadi, A.; A Idris, S. Green Synthesis of Ag, Cu and AgCu Nanoparticles using Palm Leaves Extract as the Reducing and Stabilizing Agents. In Proceedings of the IOP Conference Series: Materials Science and Engineering: 3rd International Conference on Global Sustainability and Chemical Engineering (ICGSCE), Putrajaya, Malaysia, 15–16 February 2017; IOP Publishing: Bristol, UK, 2018; p. 012063.
184. Sumbal; Nadeem, A.; Naz, S.; Ali, J.S.; Mannan, A.; Zia, M. Synthesis, characterization and biological activities of monometallic and bimetallic nanoparticles using *Mirabilis jalapa* leaf extract. *Biotechnol. Rep.* **2019**, *22*. [[CrossRef](#)]
185. Gopiraman, M.; Saravanamoorthy, S.; Baskar, R.; Ilangovan, A.; Min, C.I.; Mayakrishnan, G.; Somasundaram, S.; Ramaganthan, B. Green synthesis of Ag@Au bimetallic regenerated cellulose nanofibers for catalytic applications. *New J. Chem.* **2019**, *43*, 17090–17103. [[CrossRef](#)]
186. Binod, A.; Ganachari, S.V.; Yaradoddi, J.; Tapaskar, R.P.; Banapurmath, N.; Shettar, A.S. Biological synthesis and characterization of tri-metallic alloy (Au Ag, Sr) nanoparticles and its sensing studies. In Proceedings of the IOP Conference Series: Materials Science and Engineering: International Conference on Advances in Manufacturing, Materials and Energy Engineering (Icon MMEE 2018), Mangalore Institute of Technology & ENGINEERING, Badaga Mijar, Moodbidri, Karnataka, India, 2–3 March 2018; IOP Publishing: Bristol, UK, 2018; 376, p. 012054.
187. Sun, L.; Yin, Y.; Lv, P.; Su, W.; Zhang, L. Green controllable synthesis of Au–Ag alloy nanoparticles using Chinese wolfberry fruit extract and their tunable photocatalytic activity. *RSC Adv.* **2018**, *8*, 3964–3973. [[CrossRef](#)]
188. Rao, M.D.; Pennathur, G. Green synthesis and characterization of cadmium sulphide nanoparticles from *Chlamydomonas reinhardtii* and their application as photocatalysts. *Mater. Res. Bull.* **2017**, *85*, 64–73. [[CrossRef](#)]
189. Govindaraju, K.; Basha, S.K.; Kumar, G.; Singaravelu, G. Silver, gold and bimetallic nanoparticles production using single-cell protein (*Spirulina platensis*) Geitler. *J. Mater. Sci.* **2008**, *43*, 5115–5122. [[CrossRef](#)]
190. Scarano, G.; Morelli, E. Properties of phytochelatin-coated CdS nanocrystallites formed in a marine phytoplanktonic alga (*Phaeodactylum tricornutum*, Bohlin) in response to Cd. *Plant Sci.* **2003**, *165*, 803–810. [[CrossRef](#)]
191. Adelere, I.A.; Lateef, A. A novel approach to the green synthesis of metallic nanoparticles: The use of agro-wastes, enzymes, and pigments. *Nanotechnol. Rev.* **2016**, *5*, 567–587. [[CrossRef](#)]
192. Ali, H.R.; Hassaan, M.A. Applications of Bio-waste Materials as Green Synthesis of Nanoparticles and Water Purification. *Adv. Mater.* **2017**, *6*, 85. [[CrossRef](#)]
193. Asghar, Z.; Ahmad Poursattar, M.; Zahra, M. Agricultural waste biomass-assisted nanostructures: Synthesis and application. *Green Process. Synth.* **2019**, *8*, 421–429.
194. Zamare, D.; Vutukuru, S.S.; Babu, R. Biosynthesis of Nanoparticles from Agro-Waste: A Sustainable Approach. *In. J. Eng. App.Sci. Tech.* **2016**, *1*, 85–92.
195. Sharma, D.; Kanchi, S.; Bisetty, K. Biogenic synthesis of nanoparticles: A review. *Arab. J. Chem.* **2019**, *12*, 3576–3600. [[CrossRef](#)]
196. Newase, S.; Bankar, A.V. Synthesis of bio-inspired Ag–Au nanocomposite and its anti-biofilm efficacy. *Bull. Mater. Sci.* **2017**, *40*, 157–162. [[CrossRef](#)]
197. Ganaie, S.; Abbasi, T.; Abbasi, S. Rapid and green synthesis of bimetallic Au–Ag nanoparticles using an otherwise worthless weed *Antigonon leptopus*. *J. Exp. Nanosci.* **2015**, *11*, 1–23. [[CrossRef](#)]
198. Zhou, G.J.; Li, S.H.; Zhang, Y.C.; Fu, Y.Z. Biosynthesis of CdS nanoparticles in banana peel extract. *J. Nanosci. Nanotechnol.* **2014**, *14*, 4437–4442. [[CrossRef](#)]
199. Malik, B.; Pirzadah, T.B.; Kumar, M.; Rehman, R.U. Biosynthesis of Nanoparticles and Their Application in Pharmaceutical Industry. *Nanotechnology* **2017**, 235–252. [[CrossRef](#)]

200. Loza, K.; Heggen, M.; Epple, M. Synthesis, Structure, Properties, and Applications of Bimetallic Nanoparticles of Noble Metals. *Adv. Funct. Mater.* **2020**, *30*, 14–1909260. [[CrossRef](#)]
201. Dylla, A.G. Synthesis, Characterization and Catalytic Properties of Bimetallic Nanoparticles. Ph.D. Thesis, University of Maryland, College Park, MD, USA, 2009.
202. Tedsree, K.; Li, T.; Jones, S.; Chan, C.W.A.; Yu, K.M.K.; Bagot, P.; Marquis, E.A.; Smith, G.D.W.; Tsang, S.C.E. Hydrogen production from formic acid decomposition at room temperature using a Ag–Pd core–shell nanocatalyst. *Nat. Nanotechnol.* **2011**, *6*, 302–307. [[CrossRef](#)] [[PubMed](#)]
203. Wang, X.; Choi, S.-I.; Roling, L.T.; Luo, M.; Ma, C.; Zhang, L.; Chi, M.; Liu, J.; Xie, Z.; Herron, J.A.; et al. Palladium–platinum core-shell icosahedra with substantially enhanced activity and durability towards oxygen reduction. *Nat. Commun.* **2015**, *6*, 7594. [[CrossRef](#)] [[PubMed](#)]
204. Zhu, H.; Ke, X.; Yang, X.; Sarina, S.; Liu, H. Reduction of Nitroaromatic Compounds on Supported Gold Nanoparticles by Visible and Ultraviolet Light. *Angew. Chem. Int. Ed.* **2010**, *49*, 9657–9661. [[CrossRef](#)] [[PubMed](#)]
205. Fuku, K.; Hayashi, R.; Takakura, S.; Kamegawa, T.; Mori, K.; Yamashita, H. The Synthesis of Size- and Color-Controlled Silver Nanoparticles by Using Microwave Heating and their Enhanced Catalytic Activity by Localized Surface Plasmon Resonance. *Angew. Chem. Int. Ed.* **2013**, *52*, 7446–7450. [[CrossRef](#)]
206. Zhang, Y.; Xiao, Q.; Bao, Y.; Zhang, Y.; Bottle, S.; Sarina, S.; Zhaorigetu, B.; Zhu, H. Direct Photocatalytic Conversion of Aldehydes to Esters Using Supported Gold Nanoparticles under Visible Light Irradiation at Room Temperature. *J. Phys. Chem. C* **2014**, *118*, 19062–19069. [[CrossRef](#)]
207. Nasrabadi, H.T.; Abbasi, E.; Davaran, S.; Kouhi, M.; Akbarzadeh, A. Bimetallic nanoparticles: Preparation, properties, and biomedical applications. *Artif. Cells Nanomed. B.* **2014**, *44*, 376–380. [[CrossRef](#)]
208. Haiss, W.; Thanh, N.T.K.; Aveyard, J.; Fernig, D.G.; Hanson, J. Determination of Size and Concentration of Gold Nanoparticles from UV–Vis Spectra. *Anal. Chem.* **2007**, *79*, 4215–4221. [[CrossRef](#)]
209. Scholl, J.A.; Koh, A.L.; Dionne, J.A. Quantum plasmon resonances of individual metallic nanoparticles. *Nature* **2012**, *483*, 421–427. [[CrossRef](#)]
210. Lu, Y.; Chen, W. Sub-nanometre sized metal clusters: From synthetic challenges to the unique property discoveries. *Chem. Soc. Rev.* **2012**, *41*, 3594. [[CrossRef](#)]
211. Zheng, J.; Zhang, C.; Dickson, R.M. Highly Fluorescent, Water-Soluble, Size-Tunable Gold Quantum Dots. *Phys. Rev. Lett.* **2004**, *93*, 077402. [[CrossRef](#)]
212. Zheng, J.; Nicovich, P.R.; Dickson, R.M. Highly fluorescent noble-metal quantum dots. *Annu. Rev. Phys. Chem.* **2007**, *58*, 409–431. [[CrossRef](#)] [[PubMed](#)]
213. Zhang, S.; Metin, O.; Su, D.; Sun, S. Monodisperse AgPd Alloy Nanoparticles and Their Superior Catalysis for the Dehydrogenation of Formic Acid. *Angew. Chem. Int. Ed.* **2013**, *52*, 3681–3684. [[CrossRef](#)] [[PubMed](#)]
214. Bansmann, J.; Baker, S.; Binns, C.; Blackman, J.A.; Bucher, J.-P.; Dorantes-Dávila, J.; Dupuis, V.; Favre, L.; Kechrakos, D.; Kleibert, A.; et al. Magnetic and Structural Properties of Isolated and Assembled Clusters. *Surf. Sci. Rep.* **2005**, *56*, 189–275. [[CrossRef](#)]
215. Chen, Y.; Ding, L.; Song, W.; Yang, M.; Ju, H. Protein-specific Raman imaging of glycosylation on single cells with zone-controllable SERS effect. *Chem. Sci.* **2016**, *7*, 569–574. [[CrossRef](#)]
216. Zong, C.; Xu, M.; Xu, L.-J.; Wei, T.; Ma, X.; Zheng, X.-S.; Hu, R.; Ren, B. Surface-Enhanced Raman Spectroscopy for Bioanalysis: Reliability and Challenges. *Chem. Rev.* **2018**, *118*, 4946–4980. [[CrossRef](#)]
217. Kang, B.; Austin, L.; El-Sayed, M.A. Real-Time Molecular Imaging throughout the Entire Cell Cycle by Targeted Plasmonic-Enhanced Rayleigh/Raman Spectroscopy. *Nano Lett.* **2012**, *12*, 5369–5375. [[CrossRef](#)]
218. Martynenko, I.V.; Litvin, A.; Purcell-Milton, F.; Baranov, A.; Fedorov, A.V.; Gun'ko, Y.K. Application of semiconductor quantum dots in bioimaging and biosensing. *J. Mater. Chem. B.* **2017**, *5*, 6701–6727. [[CrossRef](#)]
219. Shukla, S.; Priscilla, A.; Banerjee, M.; Bhonde, R.R.; Ghatak, J.; Satyam, P.V.; Sastry, M. Porous Gold Nanospheres by Controlled Transmetalation Reaction: A Novel Material for Application in Cell Imaging. *Chem. Mater.* **2005**, *17*, 5000–5005. [[CrossRef](#)]
220. Wang, C.; Xu, L.; Xu, X.; Cheng, H.; Sun, H.; Lin, Q.; Zhang, C. Near infrared Ag/Au alloy nanoclusters: Tunable photoluminescence and cellular imaging. *J. Colloid Interface Sci.* **2014**, *416*, 274–279. [[CrossRef](#)]
221. Desai, M.L.; Jha, S.; Basu, H.; Singhal, R.K.; Sharma, P.; Kailasa, S.K. Chicken egg white and L-cysteine as cooperative ligands for effective encapsulation of Zn-doped silver nanoclusters for sensing and imaging applications. *Colloids Surf. A Physicochem. Eng. Asp.* **2018**, *559*, 35–42. [[CrossRef](#)]

222. Hu, H.; Huang, P.; Weiss, O.J.; Yan, X.; Yue, X.; Zhang, M.G.; Tang, Y.; Nie, L.; Ma, Y.; Niu, G.; et al. PET and NIR Optical Imaging Using Self-Illuminating 64Cu-Doped Chelator-Free Gold Nanoclusters. *Biomaterials* **2014**, *35*, 9868–9876. [[CrossRef](#)] [[PubMed](#)]
223. Nune, S.K.; Gunda, P.; Thallapally, P.K.; Lin, Y.-Y.; Forrest, M.L.; Berkland, C.J. Nanoparticles for biomedical imaging. *Expert Opin. Drug Deliv.* **2009**, *6*, 1175–1194. [[CrossRef](#)]
224. Chou, S.-W.; Liu, C.-L.; Liu, T.-M.; Shen, Y.-F.; Kuo, L.-C.; Wu, C.-H.; Hsieh, T.-Y.; Wu, P.-C.; Tsai, M.-R.; Yang, C.-C.; et al. Infrared-active quadruple contrast FePt nanoparticles for multiple scale molecular imaging. *Biomaterials* **2016**, *85*, 54–64. [[CrossRef](#)] [[PubMed](#)]
225. Yang, H.; Li, X.; Zhou, H.; Zhuang, Y.; Hu, H.; Wu, H.; Yang, S. Monodisperse water-soluble Fe–Ni nanoparticles for magnetic resonance imaging. *J. Alloy. Compd.* **2011**, *509*, 1217–1221. [[CrossRef](#)]
226. Yang, H.; Zhang, J.; Tian, Q.; Hu, H.; Fang, Y.; Wu, H.; Yang, S. One-pot synthesis of amphiphilic superparamagnetic FePt nanoparticles and magnetic resonance imaging in vitro. *J. Magn. Magn. Mater.* **2010**, *322*, 973–977. [[CrossRef](#)]
227. Maenosono, S.; Suzuki, T.; Saita, S. Superparamagnetic FePt nanoparticles as excellent MRI contrast agents. *J. Magn. Magn. Mater.* **2008**, *320*, L79–L83. [[CrossRef](#)]
228. Naha, P.C.; Lau, K.; Hsu, J.C.; Hajfathalian, M.; Mian, S.; Chhour, P.; Uppuluri, L.; McDonald, E.S.; Maidment, A.D.; Cormode, D.P. Gold silver alloy nanoparticles (GSAN): An imaging probe for breast cancer screening with dual-energy mammography or computed tomography. *Nanoscale* **2016**, *8*, 13740–13754. [[CrossRef](#)]
229. Chen, L.; Chabu, J.M.; Liu, Y.-N. Bimetallic AgM (M = Pt, Pd, Au) nanostructures: Synthesis and applications for surface-enhanced Raman scattering. *RSC Adv.* **2013**, *3*, 4391. [[CrossRef](#)]
230. Wang, J.; Ma, S.; Ren, J.; Yang, J.; Qu, Y.; Ding, D.; Zhang, M.; Yang, G. Fluorescence enhancement of cysteine-rich protein-templated gold nanoclusters using silver(I) ions and its sensing application for mercury(II). *Sens. Actuators B Chem.* **2018**, *267*, 342–350. [[CrossRef](#)]
231. Han, T.; Zhang, Y.; Xu, J.; Dong, J.; Liu, C.-C. Monodisperse AuM (M=Pt, Rh, Pd) bimetallic nanocrystals for enhanced electrochemical detection of H₂O₂. *Sens. Actuators B Chem.* **2015**, *207*, 404–412. [[CrossRef](#)]
232. Si, Y.; Bai, Y.; Qin, X.; Li, J.; Zhong, W.; Xiao, Z.; Li, J.; Yin, Y. Alkyne–DNA-Functionalized Alloyed Au/Ag Nanospheres for Ratiometric Surface-Enhanced Raman Scattering Imaging Assay of Endonuclease Activity in Live Cells. *Anal. Chem.* **2018**, *90*, 3898–3905. [[CrossRef](#)]
233. Zhai, Q.; Xing, H.; Fan, D.; Zhang, X.; Li, J.; Wang, E. Gold-silver bimetallic nanoclusters with enhanced fluorescence for highly selective and sensitive detection of glutathione. *Sens. Actuators B Chem.* **2018**, *273*, 1827–1832. [[CrossRef](#)]
234. Zhang, T.-X.; Liu, H.-J.; Chen, Y. Ultrabright gold-silver bimetallic nanoclusters: Synthesis and their potential application in cysteine sensing. *Colloids Surf. A Physicochem. Eng. Asp.* **2018**, *555*, 572–579. [[CrossRef](#)]
235. Murugavelu, M.; Karthikeyan, B. Study of Ag–Pd bimetallic nanoparticles modified glassy carbon electrode for detection of L-cysteine. *Superlattice. Microst.* **2014**, *75*, 916–926. [[CrossRef](#)]
236. Karthikeyan, B.; Murugavelu, M. Nano bimetallic Ag/Pt system as efficient opto and electrochemical sensing platform towards adenine. *Sens. Actuators B Chem.* **2012**, *163*, 216–223. [[CrossRef](#)]
237. Wang, S.; Li, J.J.; Lv, Y.; Wu, R.; Xing, M.; Shen, H.; Wang, H.; Li, L.S.; Chen, X. Synthesis of Reabsorption-Suppressed Type-II/Type-I ZnSe/CdS/ZnS Core/Shell Quantum Dots and Their Application for Immunosorbent Assay. *Nanoscale Res. Lett.* **2017**, *12*, 380. [[CrossRef](#)]
238. Ji, B.; Koley, S.; Slobodkin, I.; Remennik, S.; Banin, U. ZnSe/ZnS Core/Shell Quantum Dots with Superior Optical Properties through Thermodynamic Shell Growth. *Nano Lett.* **2020**, *20*, 2387–2395. [[CrossRef](#)]
239. Yao, D.; Liang, A.; Jiang, Z. A fluorometric clenbuterol immunoassay using sulfur and nitrogen doped carbon quantum dots. *Microchim. Acta* **2019**, *186*, 323. [[CrossRef](#)]
240. Chen, Z.; Lu, M. Novel electrochemical immunoassay for human IgG1 using metal sulfide quantum dot-doped bovine serum albumin microspheres on antibody-functionalized magnetic beads. *Anal. Chim. Acta* **2017**, *979*, 24–30. [[CrossRef](#)]
241. Wang, J.; Meng, H.-M.; Chen, J.; Liu, J.; Zhang, L.; Qu, L.; Li, Z.; Lin, Y. Quantum Dot-Based Lateral Flow Test Strips for Highly Sensitive Detection of the Tetanus Antibody. *ACS Omega* **2019**, *4*, 6789–6795. [[CrossRef](#)]
242. Huang, Z.-J.; Han, W.-D.; Wu, Y.-H.; Hu, X.-G.; Yuan, Y.-N.; Chen, W.; Peng, H.-P.; Liu, A.-L.; Lin, X. Magnetic electrochemiluminescent immunoassay with quantum dots label for highly efficient detection of the tumor marker α -fetoprotein. *J. Electroanal. Chem.* **2017**, *785*, 8–13. [[CrossRef](#)]

243. Omajali, J.B.; Gomez-Bolivar, J.; Mikheenko, I.P.; Sharma, S.; Kayode, B.; Al-Duri, B.; Banerjee, D.; Walker, M.; Merroun, M.L.; Macaskie, L.E. Novel catalytically active Pd/Ru bimetallic nanoparticles synthesized by *Bacillus benzeovorans*. *Sci. Rep.* **2019**, *9*, 4715. [[CrossRef](#)] [[PubMed](#)]
244. Wang, Y.; Zhao, Y.; Yin, J.; Liu, M.; Dong, Q.; Su, Y. Synthesis and electrocatalytic alcohol oxidation performance of Pd–Co bimetallic nanoparticles supported on graphene. *Int. J. Hydrogen Energy* **2014**, *39*, 1325–1335. [[CrossRef](#)]
245. Zhang, W.-X.; Wang, C.-B.; Lien, H.-L. Treatment of chlorinated organic contaminants with nanoscale bimetallic particles. *Catal. Today* **1998**, *40*, 387–395. [[CrossRef](#)]
246. An, C.; Kuang, Y.; Fu, C.; Zeng, F.; Wang, W.; Zhou, H. Study on Ag–Pd bimetallic nanoparticles for electrocatalytic reduction of benzyl chloride. *Electrochem. Commun.* **2011**, *13*, 1413–1416. [[CrossRef](#)]
247. Xie, H.; Ye, X.; Duan, K.; Xue, M.; Du, Y.; Ye, W.; Wang, C. CuAu–ZnO–graphene nanocomposite: A novel graphene-based bimetallic alloy-semiconductor catalyst with its enhanced photocatalytic degradation performance. *J. Alloy. Compd.* **2015**, *636*, 40–47. [[CrossRef](#)]
248. Cheng, M.; Zhu, M.; Du, Y.; Yang, P. Enhanced photocatalytic hydrogen evolution based on efficient electron transfer in triphenylamine-based dye functionalized Au@Pt bimetallic core/shell nanocomposite. *Int. J. Hydrogen Energy* **2013**, *38*, 8631–8638. [[CrossRef](#)]
249. Cai, X.-L.; Liu, C.; Liu, J.; Lu, Y.; Zhong, Y.-N.; Nie, K.; Xu, J.-L.; Gao, X.; Sun, X.-H.; Wang, S.-D. Synergistic Effects in CNTs-PdAu/Pt Trimetallic Nanoparticles with High Electrocatalytic Activity and Stability. *Nano-Micro Lett.* **2017**, *9*, 48. [[CrossRef](#)]
250. Thongthai, K.; Pakawanit, P.; Chanlek, N.; Kim, J.-H.; Ananta, S.; Srisombat, L. Ag/Au/Pt trimetallic nanoparticles with defects: Preparation, characterization, and electrocatalytic activity in methanol oxidation. *Nanotechnology* **2017**, *28*, 375602. [[CrossRef](#)]
251. Iqbal, M.T.; Halasz, K.; Bhatia, D. Metallic Nanoparticles for Targeted Drug Delivery. *Nanomater. Chem. Technol.* **2017**, *1*, 1–3.
252. Khodabandehloo, H.; Zahednasab, H.; Hafez, A.A. Nanocarriers Usage for Drug Delivery in Cancer Therapy. *Iran. J. Cancer Prev.* **2016**, *9*, 3966. [[CrossRef](#)] [[PubMed](#)]
253. Lombardo, D.; Kiselev, M.A.; Caccamo, M.T. Smart Nanoparticles for Drug Delivery Application: Development of Versatile Nanocarrier Platforms in Biotechnology and Nanomedicine. *J. Nanomater.* **2019**. [[CrossRef](#)]
254. Zhou, Q.; Zhang, L.; Wu, H. Nanomaterials for cancer therapies. *Nanotechnol. Rev.* **2017**, *6*, 473–496. [[CrossRef](#)]
255. Hossen, S.; Hossain, M.K.; Basher, M.K.; Mia, M.; Rahman, M.T.; Uddin, M.J. Smart nanocarrier-based drug delivery systems for cancer therapy and toxicity studies: A review. *J. Adv. Res.* **2018**, *15*, 1–18. [[CrossRef](#)]
256. Torchi, A.; Simonelli, F.; Ferrando, R.; Rossi, G. Local Enhancement of Lipid Membrane Permeability Induced by Irradiated Gold Nanoparticles. *ACS Nano* **2017**, *11*, 12553–12561. [[CrossRef](#)]
257. Shanmugasundaram, T.; Radhakrishnan, M.; Gopikrishnan, V.; Kadirvelu, K.; Balagurunathan, R. Biocompatible silver, gold and silver/gold alloy nanoparticles for enhanced cancer therapy: In vitro and in vivo perspectives. *Nanoscale* **2017**, *9*, 16773–16790. [[CrossRef](#)]
258. Katifelis, H.; Lyberopoulou, A.; Mukha, I.; Vityuk, N.; Grodzyuk, G.; Theodoropoulos, G.E.; Efsthathopoulos, E.P.; Gazouli, M. Ag/Au bimetallic nanoparticles induce apoptosis in human cancer cell lines via P53, CASPASE-3 and BAX/BCL-2 pathways. *Artif. Cells Nanomed. B* **2018**, *46*, S389–S398. [[CrossRef](#)]
259. Shmarakov, I.; Mukha, I.; Vityuk, N.; Borschovetska, V.; Zhyshchynska, N.; Grodzyuk, G.; Eremenko, A. Antitumor Activity of Alloy and Core-Shell-Type Bimetallic AgAu Nanoparticles. *Nanoscale Res. Lett.* **2017**, *12*, 333. [[CrossRef](#)]
260. Midha, K.; Nagpal, M.; Kalra, S. Quantum Dots in Cancer Therapy. *Int. J. Curr. Sci. Technol.* **2015**, *3*, 84–89.
261. Nafiujjaman, M.; Revuri, V.; Park, H.-K.; Kwon, I.K.; Cho, K.-J.; Lee, Y.-K. Enhanced Photodynamic Properties of Graphene Quantum Dot Conjugated Ce6 Nanoparticles for Targeted Cancer Therapy and Imaging. *Chem. Lett.* **2016**, *45*, 997–999. [[CrossRef](#)]
262. Juzenas, P.; Chen, W.; Sun, Y.-P.; Coelho, M.; Generalov, R.; Generalova, N.; Christensen, I.L. Quantum dots and nanoparticles for photodynamic and radiation therapies of cancer. *Adv. Drug Deliv. Rev.* **2008**, *60*, 1600–1614. [[CrossRef](#)]
263. Fan, H.-Y.; Yu, X.-H.; Wang, K.; Yin, Y.-J.; Tang, Y.-J.; Tang, Y.; Liang, X.-H. Graphene quantum dots (GQDs)-based nanomaterials for improving photodynamic therapy in cancer treatment. *Eur. J. Med. Chem.* **2019**, *182*, 111620. [[CrossRef](#)]

264. Martynenko, I.V.; Kuznetsova, V.; Орлова, А.О.; Kanaev, P.; Maslov, V.G.; Loudon, A.; Zaharov, V.; Parfenov, P.; Gun'ko, Y.K.; Baranov, A.V.; et al. Chlorin e6–ZnSe/ZnS quantum dots based system as reagent for photodynamic therapy. *Nanotechnology* **2015**, *26*, 55102. [[CrossRef](#)]
265. Hilger, I.; Hiergeist, R.; Hergt, R.; Winnefeld, K.; Schubert, H.; Kaiser, W.A. Thermal Ablation of Tumors Using Magnetic Nanoparticles. *Investig. Radiol.* **2002**, *37*, 580–586. [[CrossRef](#)]
266. Jose, J.; Kumar, R.; Harilal, S.; Mathew, G.E.; Parambi, D.G.T.; Prabhu, A.; Uddin, S.; Aleya, L.; Kim, H.; Mathew, B. Magnetic nanoparticles for hyperthermia in cancer treatment: An emerging tool. *Environ. Sci. Pollut. Res.* **2020**, *27*, 19214–19225. [[CrossRef](#)]
267. Maier-Hauff, K.; Rothe, R.; Scholz, R.; Gneveckow, U.; Wust, P.; Thiesen, B.; Feussner, A.; Von Deimling, A.; Waldoefner, N.; Felix, R.; et al. Intracranial Thermo-therapy using Magnetic Nanoparticles Combined with External Beam Radiotherapy: Results of a Feasibility Study on Patients with Glioblastoma Multiforme. *J. Neuro-Oncol.* **2006**, *81*, 53–60. [[CrossRef](#)]
268. DeNardo, S.J.; Miers, L.A.; Natarajan, A.; Foreman, A.R.; Gruettner, C.; Adamson, G.N.; Ivkov, R. Development of Tumor Targeting Bioprobes (111In-Chimeric L6 Monoclonal Antibody Nanoparticles) for Alternating Magnetic Field Cancer Therapy. *Clin. Cancer Res.* **2005**, *11*, 7087–7092. [[CrossRef](#)] [[PubMed](#)]
269. Xie, J.; Zhang, Y.; Yan, C.; Song, L.; Wen, S.; Zang, F.; Chen, G.; Ding, Q.; Yan, C.; Gu, N. High-performance PEGylated Mn–Zn ferrite nanocrystals as a passive-targeted agent for magnetically induced cancer theranostics. *Biomaterials* **2014**, *35*, 9126–9136. [[CrossRef](#)]
270. Xie, J.; Yan, C.; Yan, Y.; Chen, L.; Song, L.; Zang, F.; An, Y.; Teng, G.-J.; Gu, N.; Zhang, Y. Multi-modal Mn–Zn ferrite nanocrystals for magnetically-induced cancer targeted hyperthermia: A comparison of passive and active targeting effects. *Nanoscale* **2016**, *8*, 16902–16915. [[CrossRef](#)]
271. Li, Y.-Q.; Xu, M.; Dhawan, U.; Liu, W.-C.; Wu, K.-T.; Liu, X.-R.; Lin, C.; Zhao, G.; Wu, Y.-C.; Chung, R.-J. Iron–gold alloy nanoparticles serve as a cornerstone in hyperthermia-mediated controlled drug release for cancer therapy. *Int. J. Nanomed.* **2018**, *13*, 5499–5509. [[CrossRef](#)]
272. Ahamed, M.; Alhadlaq, H.A.; Khan, M.A.M.; Akhtar, M.J. Selective killing of cancer cells by iron oxide nanoparticles mediated through reactive oxygen species via p53 pathway. *J. Nanoparticle Res.* **2012**, *15*. [[CrossRef](#)]
273. Guo, Z.; Chen, Y.; Wang, Y.-H.; Jiang, H.; Wang, X. Advances and challenges in metallic nanomaterial synthesis and antibacterial applications. *J. Mater. Chem. B* **2020**, *8*, 4764–4777. [[CrossRef](#)]
274. Cheeseman, S.; Christofferson, A.J.; Kariuki, R.; Cozzolino, D.; Daeneke, T.; Crawford, R.J.; Truong, V.K.; Chapman, J.; Elbourne, A. Antimicrobial Metal Nanomaterials: From Passive to Stimuli-Activated Applications. *Adv. Sci.* **2020**, *7*, 1902913. [[CrossRef](#)]
275. Vimbela, G.V.; Ngo, S.M.; Frazee, C.; Yang, L.; Stout, D. Antibacterial properties and toxicity from metallic nanomaterials. *Int. J. Nanomed.* **2017**, *12*, 3941–3965. [[CrossRef](#)]
276. Valodkar, M.; Modi, S.; Pal, A.; Thakore, S. Synthesis and anti-bacterial activity of Cu, Ag and Cu–Ag alloy nanoparticles: A green approach. *Mater. Res. Bull.* **2011**, *46*, 384–389. [[CrossRef](#)]
277. Benetti, G.; Cavaliere, E.; Brescia, R.; Salassi, S.; Ferrando, R.; Vantomme, A.; Pallecchi, L.; Pollini, S.; Boncompagni, S.; Fortuni, B.; et al. Tailored Ag–Cu–Mg multielemental nanoparticles for wide-spectrum antibacterial coating. *Nanoscale* **2019**, *11*, 1626–1635. [[CrossRef](#)]
278. Hu, X.; Zhao, Y.; Hu, Z.; Saran, A.; Hou, S.; Wen, T.; Liu, W.; Ji, Y.; Jiang, X.; Wu, X. Gold nanorods core/AgPt alloy nanodots shell: A novel potent antibacterial nanostructure. *Nano Res.* **2013**, *6*, 822–835. [[CrossRef](#)]
279. Jiang, F.; Zhu, W.; Zhao, C.; Li, Y.; Wei, P.; Wan, T.; Ye, H.; Pan, S.; Ren, F. A strong, wear- and corrosion-resistant, and antibacterial Co–30 at.% Cr–5 at.% Ag ternary alloy for medical implants. *Mater. Des.* **2019**, *184*, 108190. [[CrossRef](#)]
280. Zhang, X.; Jiang, X.; Croley, T.R.; Boudreau, M.D.; He, W.; Cai, J.; Li, P.; Yin, J.-J. Ferroxidase-like and antibacterial activity of PtCu alloy nanoparticles. *J. Environ. Sci. Heal. Part C* **2019**, *37*, 99–115. [[CrossRef](#)]
281. Zhu, M.; Wang, R.; Nie, G. Applications of nanomaterials as vaccine adjuvants. *Hum. Vaccines Immunother.* **2014**, *10*, 2761–2774. [[CrossRef](#)]
282. Sun, B.; Xia, T. Nanomaterial-based vaccine adjuvants. *J. Mater. Chem. B* **2016**, *4*, 5496–5509. [[CrossRef](#)] [[PubMed](#)]

283. Li, X.; Aldayel, A.M.; Cui, Z. Aluminum hydroxide nanoparticles show a stronger vaccine adjuvant activity than traditional aluminum hydroxide microparticles. *J. Control. Release* **2013**, *173*, 148–157. [[CrossRef](#)] [[PubMed](#)]
284. Niikura, K.; Matsunaga, T.; Suzuki, T.; Kobayashi, S.; Yamaguchi, H.; Orba, Y.; Kawaguchi, A.; Hasegawa, H.; Kajino, K.; Ninomiya, T.; et al. Gold Nanoparticles as a Vaccine Platform: Influence of Size and Shape on Immunological Responses in Vitro and in Vivo. *ACS Nano* **2013**, *7*, 3926–3938. [[CrossRef](#)] [[PubMed](#)]



© 2020 by the authors. Licensee MDPI, Basel, Switzerland. This article is an open access article distributed under the terms and conditions of the Creative Commons Attribution (CC BY) license (<http://creativecommons.org/licenses/by/4.0/>).